Genomic epidemiology of SARS-CoV-2 in the United Arab Emirates reveals novel virus mutation, patterns of co-infection and tissue specific host innate immune response

Rong Liu[1,2], Pei Wu[1,2], Pauline Ogrodzki[1], Sally Mahmoud[1], Ke Liang[3], Pengjuan Liu[3], Stephen S. Francis[4,5], Hanif Khalak[1], Denghui Liu[6], Junhua Li[2,7], Tao Ma[3], Fang Chen[3], Weibin Liu[2], Xinyu Huang[3], Wenjun He[6], Zhaorong Yuan[6], Nan Qiao[6], Xin Meng[6], Budoor Alqarni[1], Javier Quilez[1], Vinay Kusuma[1], Long Lin[2], Xin Jin[2], Chongguang Yang[8], Xavier Anton[1], Ashish Koshy[1], Huanming Yang[2], Xun Xu[2], Jian Wang[2], Peng Xiao[1], Nawal Ahmed Mohamed Al Kaabi[9], Mohammed Saifuddin Fasihuddin[9], Francis Amirtharaj Selvaraj[9], Stefan Weber[9], Farida Ismail Al Hosani[10], Siyang Liu[2#], Walid Abbas Zaher[1#]

1. Group42 Healthcare, Abu Dhabi, United Arab Emirates

2. BGI-Shenzhen, Shenzhen 518083, Guangdong, China

3. MGI, BGI-Shenzhen, Shenzhen 518083, Guangdong, China

4. Department of Neurological Surgery, University of California, San Francisco

5. Department of Epidemiology and Biostatistics, University of California, San Francisco

6. Laboratory of Health Intelligence, Huawei Technologies Co., Ltd, Shenzhen, 518100, China

7. Shenzhen Key Laboratory of Unknown Pathogen Identification, BGI-Shenzhen, Shenzhen 518083, China

8. Department of Epidemiology of Microbial Diseases, Yale School of Public Health, New Haven

9. SEHA, Abu Dhabi Health Services Co, Abu Dhabi, United Arab Emirates

10. Department of Health, Abu Dhabi, United Arab Emirates

Correspondence to

Siyang Liu: liusiyang@bgi.com

Walid Abbas Zaher: Walid.Zaher@g42.ai

Abstract

To unravel the source of SARS-CoV-2 introduction and the pattern of its spreading and evolution in the United Arab Emirates, we conducted meta-transcriptome sequencing of 1,067 nasopharyngeal swab samples collected between May 9th and Jun 29th, 2020 during the first peak of the local COVID-19 epidemic. We identified global clade distribution and eleven novel genetic variants that were almost absent in the rest of the world defined five subclades specific to the UAE viral population. Cross-settlement human-to-human transmission was related to the local business activity. Perhaps surprisingly, at least 5% of the population were co-infected by SARS-CoV-2 of multiple clades within the same host. We also discovered an enrichment of cytosine-to-uracil mutation among the viral population collected from the nasopharynx, that is different from the adenosine-to-inosine change previously reported in the bronchoalveolar lavage fluid samples and a previously unidentified upregulation of APOBEC4 expression in nasopharynx among infected patients, indicating the innate immune host response mediated by ADAR and APOBEC gene families could be tissue-specific. The genomic epidemiological and molecular biological knowledge reported here provides new insights for the SARS-CoV-2 evolution and transmission and points out future direction on host-pathogen interaction investigation.

Keywords: SARS-CoV-2, meta-transcriptomic sequencing, phylogenetics, human-to-human transmission, co-infection, mutation spectrum and host innate immune response

Introduction

The coronavirus disease 2019 (COVID-19), caused by the infection of severe acute respiratory syndrome coronavirus 2 (SARS-CoV-2)(*1*), has become the largest outbreak since the 1918 Spanish influenza pandemic(*2*). It has resulted in 131.83 million cases and 2.86 million death, as of March, 2021(*3*). Patients infected by SARS-CoV-2 can experience a number of serious respiratory illnesses and have in many cases died from complications related to the infection(*4*). There are no specific therapeutics or fully validated vaccines available for its control to date(*5*, *6*). Dynamic transmission modelling considering seasonal variation, immunity and intervention suggests a high possibility of continuing waves of resurgence until the year 2025(*7*).

Genomic epidemiology using massively parallel high-throughput sequencing technologies (MPS) and associated analyses and bioinformatics tools have been used to understand the rapid spread and evolution of the virus at a larger scale than ever before(*8*, *9*). Public repositories including GISAID have enabled fast release and sharing of SARS-CoV-2 genome sequences(*10*). Those efforts provide valuable information to researchers and public health officials for global outbreak responses. Nevertheless, there are new questions arising regarding the virus' ongoing breadth of transmission, its evolution inter- and intra-host, as well as host-pathogen interactions. The genetic diversity of global viral strains is largely underestimated given the lack of real-time sequencing capability in most of the world, resulting in a disproportional under-study of viral populations in under- and recently-developed countries. As a consequence, there is limited information on novel and common genetic variation in those areas where virus rapidly evolves and is subjected to natural selection, as it encounters human hosts with diverse genetic background and an environment with varying temperature and humidity levels(*11*, *12*). Most published research since the start of the pandemic has focused on inter-host phylogenetics based on the assumption that only one strain of the virus is present in the sample. Intra-host viral genetic diversity and the prevalence of coinfection has not been established via sufficiently large cohort despite the possibility that it might impact clinical outcomes and potentially enable higher resolution analysis in the who-infects-whom transmission chain(*13*). Finally, while understanding how the host response to the virus will help to combat the disease, innate immune response process such as the host-dependent RNA-editing mechanism has only been investigated among limited sample cases(*14*).

The United Arab Emirates (UAE) is one of the world's most famous international hubs for business and travel and is the first country to approve a Chinese COVID-19 vaccine. Despite a long-lasting period of epidemic, only a few of the SARS-CoV-2 samples were sequenced and the transmission and evolution patterns of the virus in this area is unknown. The first case of SARS-CoV-2 was detected in the country on January 29th, 2020 (**Figure 1**). The subsequent outbreaks infected over sixty thousand individuals by the end of June 2020 and three hundred thousand individuals by the end of December 2020(*3*). Since March 2020, the UAE public health authorities have adopted a

series of strict regulations to reduce human-to-human transmission, including airport lockdown and national curfew. On the other hand, due to economic pressures, a few international flights reopened gradually in June 2020, which may be one of the reasons for the subsequent small second peak during June and August. The most outstanding third epidemic peak were observed during the December Christmas time in 2020. There have been 2-4 thousand newly confirmed cases in the country since Christmas. Since the very beginning, as a response to the pandemic, several high-throughput molecular technologies have been adopted in the UAE to extensively monitor the viral spread and for rapid screening of infected patients. A nationwide RT-qPCR screening program conducting ten thousand tests daily was launched on March 31st 2020. Almost simultaneously, a high-throughput sequencing laboratory with 12-18Tbases/day capacity was established in early April 2020, enabling meta-transcriptome sequencing of up to 192 samples in 24 hours.

To understand the transmission and infection dynamics of SARS-CoV-2 within the UAE and in relation to other countries, during April and July, 2020, we randomly collected 1,067 nasopharyngeal specimens from SARS-CoV-2 positive patients from the RT-qPCR screening program and conducted meta-transcriptomic sequencing. Our main scientific questions include (1) What is the virus genetic diversity and transmission pattern in the UAE during the first peak of the epidemic (2) What is the extent of co-infection of multiple SARS-CoV-2 variants in this international travel hub (3) Is there any innate immune host response to the SARS-CoV-2 infection that can be detected using the meta-transcriptomic sequencing, which contains both the host and the viral gene expression information.

Results

Assembly and variant detection of SARS-CoV-2 genome from deep meta-transcriptome sequencing of 1,067 nasopharyngeal swab samples

A total of 1,067 nasopharyngeal swab samples collected from SARS-CoV-2 positive patients between May 7th and June 29th 2020 in Abu Dhabi were sequenced (**Figure 1A).** Their sequencing quality metrics were summarized in **Figure S1 and Table S1**. We obtained high quality assemblies (gap proportion < 2%) for the majority of the samples (n= 896, 84.0%). In brief, using the 29891nt SARS-CoV-2 reference genome (IVDC-HB-01), we have successfully assembled all 1,067 SARS-CoV-2 consensus genomes as follows- 896 assemblies with gaps less than 500nt (gap proportion < 2%), 27 assemblies with gap less than 1000nt (gap proportion < 4%), 14 assemblies with gaps less than 1500nt (gap proportion ~5%) and 130 assemblies with gaps greater than 1500nt (**Figure 1B**). As expected, quality of the genome assemblies was closely related to the sample viral load as measured by reads per million (RPM) and qRT-PCR Ct values (**Figure 1B, Figure S2**). A set of 3 samples (id:0555, 0919 and 0945) showed low viral loads (Ct<19) with unexpectedly poor assemblies (gaps>1500nt), likely due to RNA

degradation as many of the sequenced reads were filtered out due to low complexity, i.e. high polyA proportion (**Table S1**).

The distribution of gaps identified in the sequences indicates low sequencing coverage over the 5' and the 3' ends of the genomes, which was found to be a common occurrence in all world-wide assemblies reported in GISAID. We also notice a significantly higher number of gaps around the 20,000nt position for 27.1% of the assemblies submitted to GISAID, which were not observed in our assemblies (**Figure S3**). Among the selected 896 assemblies with the highest quality (gap proportion < 2%), we identified a total of 1,245 genetic variants consisting of 698 non-synonymous and 547 synonymous variants when compared to the SARS-CoV-2 reference genome (IVDC-HB-01), (**Figure 1C**, **Table S2**). The number of variants per sample ranged from 1 to 24 with a median number of 11 (**Figure S4**). Very few genomes carried non-single nucleotide variants. There was one 2nt insertion in one sample 1069 and six deletions identified in fourteen samples 0188,0236,0252, 0290, 0305, 0339, 0512, 0536, 0757, 0758, 0761, 0763, 0785 and 1092, the largest being a 4nt deletion present in seven of the fourteen samples (**Figure S5**). The consensus variants identified from the technical replicates were exactly the same (**Table S3**), and given a 4% alternative allele frequency threshold, the concordance rate of intra-host genetic variant detection reaches 100% (**Figure S6**). The number of variants that we identified per sample did not correlate with the sequencing depth (squared pearson correlation coefficient R^2~0.02) (**Figure S7**).

Global clade composition and five novel subclades associated with eleven novel common genetic variants in the UAE SARS-CoV-2 population

Likely due to fast population expansion with a short period, we discovered that 395 out of the 896 genomes (44.1%) assembled in our study shared an identical genome sequence with at least one other assembled genome (**Table S4**). For the purpose of downstream phylogenetic analysis, we filtered the 896 genome sequences as to keep only unique sequences, resulting in 637 unique genome sequences. We constructed a maximum likelihood phylogenetic tree including, 1) the 637 SARS-CoV-2 unique genomes and collected assembled in our study between May 7th and June 29th 2020 in Abu Dhabi, 2) the 52 nearest relative world-wide genomes identified from GISAID between February 2nd and April 24th 2020 (**Table S6, Figure S8**), and 3) 25 genomes collected from the nearby Dubai Emirate between January 29th and March 18th 2020 (*15*) . We identified the five dominant clades worldwide (*16*, *17*) in the UAE viral population sequenced in this study **(Figure 2A)**. A total of 13 (2.04%) and 140 viral genomes (21.98%) out of the 637 genomes were clustered as clade 19A and clade 19B, respectively, the two earliest clades first reported in China, Asia(*18*), while the rest of the genomes sequences were classified in the clades 20A (N=52, 8.16%), 20B (N=428, 67.19%) and 20C (N=4, 0.63%), which were first reported and became prevalent in Europe and North America[4,16]. Three samples in clade 19A, i.e. samples 0134, 0135 and 0565, harbored a higher number of mutations; 20, 19 and 19, respectively, compared to

177 the calculated average of 11 variants per genome. The closest strain found to these
178 three samples was SARS-CoV-2 USA/WA-S771/2020 reported in Washington, DC,
179 United States on April 13th, 2020 (**Table S6**). The high level of mutations occurring in
180 these samples compared to the rest of the UAE genomes, indicates a different
181 introduction of strains within the same clade.

182 There were five large sub-clades involving more than half of the collected samples
183 (381 out of the 637 unique viral genomes, 59.81%) (**Figure 2A)**, differentiated by eleven
184 mutations that were common in the UAE viral population (allele frequency > 5%) and that
185 were significantly less common among the worldwide viral population (P < 3.94e-82,
186 Fisher exact test) (**Figure 2B, Table 1**). The five sub-clades were (1) 19B.1 which
187 consisted of 17.27% of the 637 UAE unique samples, harboring the G28878A, G29742A,
188 G11230T and G28167A mutations; (2) 20B.1 which consisted of 8.48% of the samples,
189 harboring the T7171C and C27002T mutations; (3) 20B.2 which consisted of 19.15% of
190 the samples, harboring the T21775G and G5924A mutations; (4) 20B.3 which consisted
191 of 8.95% of the samples, harboring the G23311T mutation and (5) 20B.4 which
192 consisted of 5.97% of the samples, harboring the C7851T and the A24170G mutations.

193 Fortunately, individuals classified as carrying certain subclades of the virus did not
194 display significantly different viral loads in their samples as reflected by the RT-qPCR Ct
195 values (**Figure 3**). These 11 variants that defined the subclades tend to occur in highly
196 conserved regions within the SARS-CoV-2 genome (**Figure S9**). Molecular dynamic
197 analysis of two of the missense variants in the spike protein did not suggest substantially
198 different change of the protein structure between the mutant and the wildtype (**Figure**
199 **S10, Table S7**). Likely due to a recent occurrence, the temporal change of the mutation
200 allele frequency for the subclade-definitive variants is smaller compared to the
201 clade-definitive variants (**Figure S11-S12**).

202

203 **Cross-settlement human-to-human transmission contributes to the UAE epidemic**

204 We further investigated human-to-human transmission across 14 settlements from
205 three regions in the Abu Dhabi Emirate and 1 settlement in the Dubai Emirate by
206 constructing the transmission network for 120 samples with geographical and sampling
207 date information (**Figure 4A**). The constructed transmission network indicates prevalent
208 cross-settlement human-to-human transmissions contributing to the epidemic, as within
209 each clade or sub-clade, samples from multiple geographical areas were observed
210 (**Figure 4B**). We also determined the genetic distance using the L1-norm metric that
211 utilized intra-host genetic variation rather than merely the consensus genetic variation,
212 among longitudinal samples (n=24) defined as, same individuals (n=7) sampled multiple
213 times (avg=5.2) over a determined period of time (avg= 4.06 days), and among samples
214 from the same and varying settlements (**Figure 4C**). The median L1-norm genetic
215 distance was smallest among the 24 samples within the longitudinal sampling period,
216 suggesting high levels of stability in viral composition within the same host. As expected,

most samples within the same settlement had a genetic distance smaller than the cross-area distance with only two exceptions - samples from the Ghayathi settlement in the Al-Dhafra region and samples from Khabisi in the Dubai emirate, that displayed the largest genetic distance. This is consistent with the fact that those two settlements were relatively less populous compared to the settlements in the Abu Dhabi and Al-Ain regions. The spectrum and the scale of the L1-norm genetic distance is much larger than the genetic computed from the consensus genetic variants although the haplotype information is missing. Due to the small scale of sampling, we didn't further resolve the transmission network to a finer scale.

Prevalent co-infection by multiple SARS-CoV-2 variants in the same host

The international hub status of the UAE provides a good opportunity to study the prevalence of multiple SARS-CoV-2 variant co-infection within the same host. We have identified a total of 1,268 intra-host single nucleotide variation (iSNV, with minor allele count of 4 and minor allele frequency greater than 5%) present in 625 out of the 896 samples, ranging from 1 to 26 iSNV per individual with an average of one per individual (**Figure S13**). Although the technical replicates indicate 100% concordance of the iSNV detection at the above threshold, we chose a conservative way of evaluating the prevalence of multiple infection present in the sampled viral population by restricting the definition of co-infection by the co-occurrence of two clades including 19A, 19B, 20A, 20B and 20C (classified using the eleven clade-definitive variants in Figure 2) or subclades (classified using the other eleven sub-clade definitive variants) in the same sample. We found that a total of 48 samples out of the 896 (5%) carried viral variants from more than two distinct clades or subclades (**Figure 5**). The high linkage disequilibrium of the genetic variants that belong to a specific clade indicates the likely presence of a viral variant rather than spontaneous *de novo* mutations. Notably, two of the samples (id: 0855 and 0796) with identical consensus sequence displayed different patterns of multiple infection. Sample 0796 harbored viral genetic variants from clades 19A, 20A, 20B while 0855 harbored variants from clades 20A, and 20B and not from 19A. Samples in the same clade classified by the consensus variants also demonstrate a different pattern of co-infection. For example, for samples in clade 19B, two clusters were observed. One consists of seven samples with multiple infections from several clades (19A, 19B, 20A, 20B) and the other cluster consists of ten samples co-infected with 19B and 20A. For the most prevalent clade 20B viral sub-population, samples could be co-infected by 19A or 20C. Those patterns in Figure 5A largely maintain when using a 0.5% minor allele frequency threshold and the same 4 minor allele support (**Figure S14-S15**), showing a tremendous amount of intra-host genetic diversity underlying the consensus genomes of the host.

The innate immune host response to SARS-CoV-2 infection may be tissue-specific and associated with the upregulated gene expression of *APOBEC4*

We further investigated detectable innate immune host response to SARS-CoV-2 infection utilizing information that can be extracted from the meta-transcriptomic sequencing. A recent publication by Giorgio *et al*. reported evidence of RNA editing in bronchoalveolar lavage fluid (BALF) from eight patients diagnosed with SARS-CoV-2 infection in Wuhan city, China(*19*). For seven out of the eight samples, they identified a bias of the mutation towards transition, mainly A>G/T>C changes followed by C>T/G>A changes, indicating a deamination effect introduced by ADARs and APOBECs, respectively (**WH BALF in Figure 6A**). In the nasopharyngeal swab sampling of 896 patients in our study, on the contrary, we identified the C>T/G>A as the predominant SNV type that were more likely to be mediated by APOBEC gene family rather than the A>G/T>C effects mediated by the ADARs (**UAE in Figure 6A**). This held true when only mutations that occurred in more than two patients were considered. As expected, the C-to-U changes are biased toward the positive strand, i.e. more C-to-U was observed compared to G-to-A, as APOBECs are supposed to target single stranded RNA(*20*). The observation of a dominant C-to-U changes were replicated in the nasopharyngeal swab samples collected in Spain, Virginia and Ruijin hospitals in Shanghai city, China and the 23,164 high quality sequences collected in GISAID (Supplementary notes), which consistently displayed an enrichment in the C>T/G>A mutations, same as the pattern in the UAE nasal swab samples but different from the Chinese BALF results reported by Giorgio *et al (**Figure 6A**)*. Additional evidence can be obtained with the observation of cytosine depletion in viral sequences during the past ten months, reflected by an increasing of T and A bases and a decreasing of G and C bases (**Figure S16**).

We further investigated if the different patterns observed could be due to the differential gene expression of the *APOBEC* gene families and *ADAR* in the nasopharyngeal swab vs. BALF using public multi-tissue gene expression information from GTEx repository(*21*) and by analyzing the gene expression of *APOBEC* and *ADAR* genes in our sequencing data. According to the GTEx gene expression data among 49 tissues and cells, *ADAR* demonstrated the highest gene expression compared to *APOBEC* gene family in the lung and in the minor salivary gland, the two most relevant tissue compared to the nasopharynx used in our study (**Figure S17**). The GTEx information cannot directly explain the different mutation pattern between the BALF and the nasal swab samples.

Distinct from the GTEx profile obtained from the uninfected individuals (Figure S17), *APOBEC4（A4）* displayed the highest average gene expression in the nasal swab samples collected in our study, followed by *ADAR* and *APOBEC3A*, while there were very few samples expressed *APOBEC1*, *APOBEC2* and *APOBEC3H* (**Figure 6B**) . The difference of gene expression is significant between *A4* and the *ADAR* (Wilcoxon test P=7.7e-05) and the largest difference was observed among the individuals carrying clade 20A variants followed by the clade 19B variants (**Figure 6B**, **Table S8**). In GTEx,

298 *A4* is expressed most prominently in testis, lowly expressed in lung and infrequently
299 expressed in other tissues (**Figure S17**).

300 The significantly up-regulated *A4* gene expression in the nasopharynx could have
301 been triggered by the SARS-CoV-2 infection. A4 was an under-studied putative
302 cytidine-to-uridine editing enzyme, which cytidine deaminase activity was not as
303 well-known as the APOBEC3A(*22*). The sequencing data not aligned to the
304 SARS-CoV-2 were filtered out from the BALF samples and therefore, we were not able
305 to investigate the gene expression of those host genes in this tissue. That the A4 was
306 previously reported to enhance the replication of HIV-1 indicates its involvement against
307 the RNA virus infection. The high expression of *A4* in nasopharynx may provide the first
308 evidence that the enzyme may be involved as part of the host responses upon the
309 SARS-CoV-2 infection and further experimental analysis is worthwhile to understand its
310 exact functions.

311

312 Discussion

313 Our analysis of the 1,067 viral genomes collected in the UAE suggest that, during the
314 first quarter of 2020, there were multiple and likely independent introductions of
315 SARS-COV-2. The five dominant global clades of SARS-CoV-2 were all commonly
316 present in the sampled individuals (Figure 2**)**. The highest prevalence of the European
317 dominant clade 20B, followed by the East Asian dominant clade 19B, indicates effects of
318 either a larger founder population size or positive selection. There was substantial local
319 transmission within and between areas in the Abu Dhabi emirate (Figure 4). We have
320 identified 5 new sub-clades, namely; 19B.1, 20B.1, 20B.2, 20B.3 and 20B.4, defined by
321 11 variants uniquely found within the UAE. Those variants are potentially neutral given
322 that no significantly different viral loads (reflected by the RT-qPCR test) were detected
323 between patients carrying the subclades and those did not (Figure 3).

324 While consensus sequences tend to be highly similar, intra-host variation adds
325 information which is a promising novel direction for resolving finer-scale transmission
326 networks and studying co-infection of the patients. This study offers the first insight into
327 the prevalence of co-infections of multiple SARS-CoV-2 strains in a large cohort. We
328 observed that at least 5% of the patients were infected by more than one SARS-CoV-2
329 strain. Within-host co-infection of SARS-CoV-2 variants has been reported in very few
330 studies and with limited sample size. The environment created by the UAE's
331 "international hub" status also enables a reliable approach to study co-infection within an
332 individual by different strains of SARS-CoV-2 using clade and sub-clade definitive
333 genetic variants. This raises the importance of carefully collecting valuable
334 epidemiological data worldwide, on the origin and clinical relevance of the multiple
335 infections, and the possibility of further granularity when studying transmission dynamics
336 by utilizing information from multiple strains.

While this study showed that SARS-CoV-2 successfully mutated in the two-month period collection in the United Arab Emirates, it is clear that a large number of mutational changes have taken place in the past 10 months of this pandemic. This would likely result in an immunologic battle between host response and changes in the viral genome potentially leading to important structural changes. We observed a significant accumulation of C-to-U mutations in the nasopharyngeal swab samples collected in this study compared to the early stages of sampling around the globe. This pattern is different to what has been reported in a recent study where an enrichment of A-to-G was followed by T-to-C mutations in seven out of eight BALF samples from Wuhan(*19*). We suspect that tissue-specific gene expression of ADAR and member of the APOBEC protein family may contribute to this observation and discovered that *APOBEC4* was highly expressed in the nasopharynx. Given that APOBEC4 was previously reported to enhance RNA virus replication and was mainly expressed in Testis in an ordinary status, it will be interesting and worthwhile to understand more about its exact function towards the SARS-CoV-2 infection using experimental analysis.

The genomic epidemiological insights from our study will provide a strong basis for the surveillance of emerging mutations within the local viral population. Following the gradual reopening of borders and worldwide travels, the continuous sequencing and identification of allele frequency changes of those variants and additional experimental validation are necessary to verify their biological impacts. Future efforts will be aimed at speeding up the process in providing near real-time molecular surveillance and in the coordination of epidemiological and genomic data to rapidly adapt to SARS-CoV-2 evolution to ensure public safety, adequate diagnosis and accurate pharmaceutical development.

Methods

Study design and population

Patients with positive RT-qPCR SARS-COV-2 diagnosis are referred to local designated hospitals administered by the Abu Dhabi Health Services Co (SEHA) and the Department of Health in Abu Dhabi (DOH) for quarantine and treatment. Through a routine surveillance system, all cases of SARS-CoV-2 are reported to the DOH.

In this population-based retrospective study, we have randomly selected 1,067 patients testing positive for SARS-CoV-2 during the months of May and June 2020, regardless of their clinical symptoms. We collected the nasopharyngeal swab samples of the patients from the population screening program and sent them to G42 Biogenix laboratory for RNA extraction using the MGIEasy Magnetic Beads Virus DNA/RNA Extraction Kit (MGI, Shenzhen, China) on MGISP-960 (MGI, Shenzhen, China). Real-time quantitative PCR (RT-qPCR) was used to quantify viral abundance in the sample, determined by Ct values. The electronic epidemiological meta-data was provided by the DOH using the case report form. The study was approved by the Abu

377 Dhabi COVID19 Research IRB Committee (approval number DOH/CVDC/2020/1945).
378 All analyses were performed on the G42 Health AI computational platform
379 (https://www.g42health.ai/) under local data security and privacy regulations.

380 **Classification of the SARS-CoV-2 reads from the meta-transcriptome sequencing**

381 Classification, *de novo* assembly and consensus variation detection of the
382 SARS-CoV-2 generally follow the protocol in our previous study[15]. Briefly, total reads
383 were processed using Kraken v0.10.5 (default parameters) with a self-built database of
384 Coronaviridae genomes (including SARS, MERS, and SARS-CoV-2 genome sequences
385 downloaded from GISAID, NCBI, and CNGB) to identify Coronaviridae-like reads in a
386 sensitive manner. Fastp v0.19.5 (parameters: -q 20 -u 20 -n 1 -l 50) and SOAPnuke
387 v1.5.6 (parameters: -l 20 -q 0.2 -E 50 -n 0.02 -5 0 -Q 2 -G -d) were used to remove
388 low-quality reads, duplications, and adaptor contaminations. Low-complexity reads were
389 then removed using PRINSEQ v0.20.4 (parameters: -lc_method dust -lc_threshold 7).

390 **Alignment to reference genome**

391 Reads aligned to SARS-CoV-2 reference genome
392 (BetaCoV/Wuhan/IVDC-HB-01/2019|EPI_ISL_402119) were classified as
393 SARS-CoV-2 reads. Sequencing depth was measured using samtools depth using the
394 default parameters. Samples that exhibited 10-fold average sequencing depth after
395 filtration were accepted for downstream analyses. Reads per million (RPM) belonging to
396 the SARS-CoV-2 was estimated by dividing the reads aligned to SARS-CoV-2 by the
397 total number of reads generated from the same sample.

398 **Genome assembly**

399 The BetaCoV/Wuhan/IVDC-HB-01/2019|EPI_ISL_402119 sequence was used as
400 the virus reference genome. The IVDC-HB-01 reference lacks 12 A nucleotides at the
401 end compared to Wuhan/Hu-1/2019 and consists of 24 more sequences at the 5'
402 beginning compared to Wuhan/WH01/2019. SARS-CoV-2 consensus sequences were
403 generated using Pilon v1.23 (parameters: --changes –vcf --changes --vcf --mindepth 10
404 --fix all, amb)[16]. Nucleotide positions with sequencing depth < 10× were masked as
405 ambiguous base N. We have also applied *de novo* assembly of the Coronaviridae-like
406 reads from samples with < 100× average sequencing depth using SPAdes (v3.14.0) with
407 the default settings. The Coronaviridae-like reads of samples with > 100× average
408 sequencing depth across SARS-CoV-2 genome were subsampled to achieve 100×
409 sequencing depth before being assembled. However, the assembled genomes are
410 enriched of errors and therefore we didn't use those assembled sequences in the
411 downstream analysis.

412 **Consensus variation detection and annotation**

413 Pilon generates a variant calling formatted file for recording the consensus variation.
414 To verify the correctness of those consensus variation calls, we also applied freebayes
415 (v1.3.1) (parameters: -p 1 -q 20 -m 60 --min-coverage 10 -V) to detect genetic variation

from the bam file. The low-confidence variants were removed with snippy-vcf_filter (v3.2) (parameters: --minqual 100 --mincov 10 --minfrac 0.8). The correctness of those results was evaluated using the two technical replicates (**Table S3**). The remaining variants in VCF files generated by freebayes were annotated in SARS-CoV-2 genome assemblies and consensus sequences with SNVeff (v4.3) using default parameters[17]. Jalview (v1.8.3) was used to perform multiple sequence alignment and estimate the conservativeness score of the mutations[18].

Intra-host variation detection

We applied reditools[19] to compute the sequencing depth of the four A, C, G, T bases (parameters: python2.7 reditools.py -f sample.bam -o sample.count.txt -S -s 0 -os 4 -r ref.fa -q 25 -bq 35 -mbp 15 -Mbp 15). The intra-host genetic variation was detected using reditools(*24*) with a minimum frequency of 5% and 4 copies of minor alleles. We have applied three technical replicates for two samples to evaluate the accuracy of the assembled sequence, the consensus and intra-host genetic variants. This conservative cutoff was decided based on the two sets of technical replicates with examination of concordance (SNV found in both samples) and discordance (SNV found in only one of the two samples) for different frequency thresholds.

L1-norm genetic distance

We calculate the L1 norm genetic distance by comparing each variant nucleotide position of two samples.

$$\mathrm{d_k(p, q)} = \sum_{i=1}^{n} |p_i - q_i|$$

We define d_k as the distance measured at position k for comparing samples p and q, and n is the total number of possible nucleotide configurations (A, C, G, T) to calculate the difference in frequency of the same nucleotide in different two samples. For each pair of samples, we use D to represent the sum of the degree of difference in all positions, and N is the sum of the number of variant nucleotides in the two samples.

$$\mathrm{D} = \sum_{\mathrm{k}=1}^{\mathrm{N}} \mathrm{d_k}$$

This single number D quantifies the degree of difference in all nucleotide variants between the two samples. We repeated this process for all samples.

Analysis of host ADAR and APOBEC gene expression

Reads were aligned to the human genome reference (GRCh38) using hisat2 (parameters: --phred64 --no-discordant --no-mixed -I 1 -X 1000 -p 4). Reads aligned to the exons defined by UCSC (gencode.v29.annotation.gtf) were counted (parameters: -s no -f bam -t exon -m union -r name -i gene_id). TPM was defined by the following formula where

$$TPM(x) = \frac{C_x \times r \times 10^6}{L_x \times T} = \frac{C_x/L_x \times 10^6}{\sum_{i=1}^{N} C_i/L_i}$$

where x refers to a gene or a transcript. R refers to the read length, C_x indicates the number of read pairs aligned to the exons of the gene x. T indicates the length of the gene (kb) divided by the total length of all the genes (kb). L_x indicates the length of gene x.

Phylogenetic analysis and cross-area transmission inference

From the total 896 assembled high-quality genomes (<2% gap proportion), 637 were unique, therefore considered as different strains, and were used for further phylogenetic analysis. These were aligned to 46,917 genome sequences collected outside of the UAE between January 10th and June 16th 2020 and deposited to the GISAID EpiCoV database (https://www.epicov.org/).

As subset of genome sequences were selected for phylogenetic tree building, including the 637 strains sequenced in this study, the 52 most closely related genome sequences from the alignment analysis against the global 46,917 sequences, and 25 genome sequences also obtained from GISAID that were collected and sequenced in Dubai, UAE, from January 29th to March 15th 2020. We built a maximum likelihood phylogenetic tree using the Nextstrain pipeline; Augur v6.4.3 and MAFFT v7.455 for multiple sequence alignment and IQtree v1.6.12 for phylogenetic tree construction (*25*). FigTree v1.4.4 was used to visualize and annotate the phylogenetic tree. Clades were defined following the Nextstrain nomenclature(*16*). Subclades were further defined in this study based on common variants (>5%) in the UAE but is significantly rarely present in the rest of the world (fisher exact p-value < 4e-82).

Samples with corresponding epidemiological data including patients' addresses and date of first sample collection were also used to generate median-joining networks for each clades and subclades using PopART (Population Analysis with Reticulate Trees) v1.7. L1-norm genetic distance was computed using the formula previously defined in the influenza study by Poon, *et al* (2016)(*13*), reflecting the sum of the degree of difference for each variant nucleotide position of any two samples.

Statistical analysis

Fisher exact tests were applied to the 637 unique genomes identified in this study and to 23,164 SARS-CoV-2 genomes collected worldwide from GISAID and curated in the China National Center for Bioinformation (CNCB)(*26*). The tests were used to identify variants that display substantial allele frequency differences between the two sets of genomes sequences; UAE vs. rest of the world. Kruskai-Wallis test was used to compare the RT-qPCR Ct values between clades and subclades.

The distribution of the 10 types of genetic mutations (e.g. A>C, C>G mutations) as well as the base contents for all 4 nucleotides (A, C, G and U) as a function of time was

used to infer the RNA-editing functions of ADAR and APOBEC proteins within the host. The enrichment of a specific type of mutations were tested using chisq tests.

Mutation analysis related to the host response

The URL for data resources in investigating the nucleotide changes from Ruijin, Virginia, Spain, Wuhan and GISAID were detailed in Supplementary notes.

Molecular Dynamics Simulation

The original structures (PDB format) of SARS-CoV-2 proteins were downloaded from Protein Data Bank (PDB, https://www.rcsb.org/) with accession numbers, ORF3a: 6xdc, Spike: 6vyb and NSP12:7bv2. Point mutations were introduced into each protein sequence and generated the mutated sequence. The mutated sequence and the corresponding original template protein structure were then taken as inputs for SWISS-MODEL for Homology modeling. After the modeling was completed, the PDB files of the target mutated proteins were obtained for further analysis. Subsequently, Ions and waters are deleted from PDB files. The PDB files were then subjected to GROMACS (Version: V5.1) and utilized for molecular dynamics simulation at the temperature 300K. Gromacs output the free energy (KJ/mol) to measure the stability of candidate protein. A smaller value of free energy indicates a higher stability of protein.

Role of the funding source

The funding source of the study had no role in the study design, data collection, data analysis, data interpretation, or writing of the report. The corresponding author had full access to all the data in the study and had final responsibility for the decision to submit for publication.

Data availability

A total of 896 high quality consensus assemblies (with less than 2% gaps) were submitted to GISAID (EPI_ISL_698105-698169, EPI_ISL_698172-699161, EPI_ISL_708827-708838) and raw sequencing data aligned to the SARS-CoV-2 reference genome were uploaded to NCBI (PRJNA687136) . We combined our genomes with other publicly available sequences for a final dataset of 973 SARS-CoV-2 genomes(ncov_global.json, Supplementary file). The dataset can be visualized on the ‘‘community’’ Nextstrain page.

Reference

1. N. Zhu, D. Zhang, W. Wang, X. Li, B. Yang, J. Song, X. Zhao, B. Huang, W. Shi, R. Lu, P. Niu, F. Zhan, X. Ma, D. Wang, W. Xu, G. Wu, G. F. Gao, W. Tan, A Novel Coronavirus from Patients with Pneumonia in China, 2019. N. Engl. J. Med. (2020), doi:10.1056/nejmoa2001017.

2. N. P. A. S. Johnson, J. Mueller, Updating the accounts: global mortality of the 1918-1920 《Spanish》 influenza pandemic. Bull. Hist. Med. (2002), doi:10.1353/bhm.2002.0022.

3. John Hopkins University and Medicine, COVID-19 Map - Johns Hopkins Coronavirus Resource Center. John Hopkins Coronavirus Resour. Cent. (2020).

4. W. Guan, Z. Ni, Y. Hu, W. Liang, C. Ou, J. He, L. Liu, H. Shan, C. Lei, D. S. C. Hui, B. Du, L. Li, G. Zeng, K. Y. Yuen, R. Chen, C. Tang, T. Wang, P. Chen, J. Xiang, S. Li, J. L. Wang, Z. Liang, Y. Peng, L. Wei, Y. Liu, Y. H. Hu, P. Peng, J. M. Wang, J. Liu, Z. Chen, G. Li, Z. Zheng, S. Qiu, J. Luo, C. Ye, S. Zhu, N. Zhong, Clinical characteristics of coronavirus disease 2019 in China. N. Engl. J. Med. (2020), doi:10.1056/NEJMoa2002032.

5. O. Ashraf, A. Virani, T. Cheema, COVID-19: An Update on the Epidemiological, Clinical, Preventive, and Therapeutic Management of 2019 Novel Coronavirus Disease. Crit. Care Nurs. Q. (2021), doi:10.1097/CNQ.0000000000000346.

6. L. T. Giurgea, M. J. Memoli, Navigating the Quagmire : Comparison and Interpretation of COVID-19 Vaccine Phase 1 / 2 Clinical Trials, 1–13 (2020).

7. S. M. Kissler, C. Tedijanto, E. Goldstein, Y. H. Grad, M. Lipsitch, Projecting the transmission dynamics of SARS-CoV-2 through the postpandemic period. Science. 368, 860–868 (2020).

8. T. Bedford, A. Greninger, P. Roychoudhury, L. Starita, M. Famulare, M.-L. Huang, A. Nalla, G. Pepper, A. Reinhardt, H. Xie, L. Shrestha, T. Nguyen, A. Adler, E. Brandstetter, S. Cho, D. Giroux, P. Han, K. Fay, C. Frazar, M. Ilcisin, K. Lacombe, J. Lee, A. Kiavand, M. Richardson, T. Sibley, M. Truong, C. Wolf, D. Nickerson, M. Rieder, J. Englund, J. Hadfield, E. Hodcroft, J. Huddleston, L. Moncla, N. Müller, R. Neher, X. Deng, W. Gu, S. Federman, C. Chiu, J. Duchin, R. Gautom, G. Melly, B. Hiatt, P. Dykema, S. Lindquist, K. Queen, Y. Tao, A. Uehara, S. Tong, D. MacCannell, G. Armstrong, G. Baird, H. Chu, J. Shendure, K. Jerome, Cryptic transmission of SARS-CoV-2 in Washington State. Science (80-.). (2020), doi:10.1101/2020.04.02.20051417.

9. D. S. Candido, I. M. Claro, J. G. de Jesus, W. M. Souza, F. R. R. Moreira, S. Dellicour, T. A. Mellan, L. du Plessis, R. H. M. Pereira, F. C. S. Sales, E. R. Manuli, J. Thézé, L. Almeida, M. T. Menezes, C. M. Voloch, M. J. Fumagalli, T. M. Coletti, C. A. M. da Silva, M. S. Ramundo, M. R. Amorim, H. H. Hoeltgebaum, S. Mishra, M. S. Gill, L. M. Carvalho, L. F. Buss, C. A. Prete, J. Ashworth, H. I. Nakaya, P. S. Peixoto, O. J. Brady, S. M. Nicholls, A. Tanuri, Á. D. Rossi, C. K. V. Braga, A. L. Gerber, A. P. C. de Guimarães, N. Gaburo, C. S. Alencar, A. C. S. Ferreira, C. X. Lima, J. E. Levi, C. Granato, G. M. Ferreira, R. S. Francisco, F. Granja, M. T. Garcia, M. L. Moretti, M. W. Perroud, T. M. P. P. Castiñeiras, C. S. Lazari, S. C. Hill, A. A. de Souza Santos, C. L. Simeoni, J. Forato, A. C. Sposito, A. Z. Schreiber, M. N. N. Santos, C. Z. de Sá, R. P. Souza, L. C. Resende-Moreira, M. M. Teixeira, J. Hubner, P. A. F. Leme, R. G. Moreira, M. L. Nogueira, N. M. Ferguson, S. F.

563 Costa, J. L. Proenca-Modena, A. T. R. Vasconcelos, S. Bhatt, P. Lemey, C. H. Wu,
564 A. Rambaut, N. J. Loman, R. S. Aguiar, O. G. Pybus, E. C. Sabino, N. R. Faria,
565 Evolution and epidemic spread of SARS-CoV-2 in Brazil. Science (80-.). (2020),
566 doi:10.1126/SCIENCE.ABD2161.

567 10. GISAID, GISAID Initiative. Adv. Virus Res. (2020).

568 11. B. Korber, W. M. Fischer, S. Gnanakaran, H. Yoon, J. Theiler, W. Abfalterer, N.
569 Hengartner, E. E. Giorgi, T. Bhattacharya, B. Foley, K. M. Hastie, D. G. Parker,
570 Tracking changes in SARS-CoV-2 Spike: evidence that D614G increases
571 infectivity of the COVID-19 virus. Cell, 1–16 (2020).

572 12. Y. C. F. Su, D. E. Anderson, B. E. Young, M. Linster, F. Zhu, J. Jayakumar, Y.
573 Zhuang, S. Kalimuddin, J. G. H. Low, C. W. Tan, W. N. Chia, T. M. Mak, S.
574 Octavia, J. M. Chavatte, R. T. C. Lee, S. Pada, S. Y. Tan, L. Sun, G. Z. Yan, S.
575 Maurer-Stroh, I. H. Mendenhall, Y. S. Leo, D. C. Lye, L. F. Wang, G. J. D. Smith,
576 Discovery and genomic characterization of a 382-nucleotide deletion in ORF7B
577 and orf8 during the early evolution of SARS-CoV-2. MBio. 11, 1–9 (2020).

578 13. L. L. M. Poon, T. Song, R. Rosenfeld, X. Lin, M. B. Rogers, B. Zhou, R. Sebra, R. A.
579 Halpin, Y. Guan, A. Twaddle, J. V. DePasse, T. B. Stockwell, D. E. Wentworth, E.
580 C. Holmes, B. Greenbaum, J. S. M. Peiris, B. J. Cowling, E. Ghedin, Quantifying
581 influenza virus diversity and transmission in humans. Nat. Genet. (2016),
582 doi:10.1038/ng.3479.

583 14. M. A. O'Connell, N. M. Mannion, L. P. Keegan, The Epitranscriptome and Innate
584 Immunity. PLoS Genet. (2015), , doi:10.1371/journal.pgen.1005687.

585 15. A. A. Tayoun, T. Loney, H. Khansaheb, S. Ramaswamy, D. Harilal, Z. O. Deesi, R.
586 M. Varghese, H. Al Suwaidi, A. Alkhajeh, L. M. AlDabal, M. Uddin, R. Hamoudi, R.
587 Halwani, A. Senok, Q. Hamid, N. Nowotny, A. Alsheikh-Ali, Multiple early
588 introductions of SARS-CoV-2 into a global travel hub in the Middle East. bioRxiv
589 (2020).

590 16. A. Rambaut, E. C. Holmes, V. Hill, A. OToole, J. McCrone, C. Ruis, L. du Plessis,
591 O. Pybus, Nat. Miocrobiology, in press, doi:10.1101/2020.04.17.046086.

592 17. Nextstrain, Genomic epidemiology of novel coronavirus - Global subsampling.
593 nextstrain.org (2020).

594 18. X. Tang, C. Wu, X. Li, Y. Song, X. Yao, X. Wu, D. Duan, H. Zhang, Y. Wang, Z.
595 Qian, J. Cui, On the origin and continuing evolution of SARS-CoV-2 | National
596 Science Review | Oxford Academic. Natl. Sci. Rev. (2020).

597 19. S. Di Giorgio, F. Martignano, M. G. Torcia, G. Mattiuz, S. G. Conticello, Evidence
598 for host-dependent RNA editing in the transcriptome of SARS-CoV-2. Sci. Adv.
599 (2020), doi:10.1126/sciadv.abb5813.

600 20. R. S. Harris, J. P. Dudley, APOBECs and virus restriction. Virology (2015), ,
601 doi:10.1016/j.virol.2015.03.012.

602 21. L. J. Carithers, H. M. Moore, The Genotype-Tissue Expression (GTEx) Project.
603 Biopreserv. Biobank. (2015), , doi:10.1089/bio.2015.29031.hmm.

604 22. J. D. Salter, R. P. Bennett, H. C. Smith, The APOBEC Protein Family: United by
605 Structure, Divergent in Function. Trends Biochem. Sci. (2016), ,
606 doi:10.1016/j.tibs.2016.05.001.

607 23. R. Drmanac, B. A. Peters, G. M. Church, C. A. Reid, X. Xu, Accurate whole
608 genome sequencing as the ultimate genetic test. Clin. Chem. (2015),
609 doi:10.1373/clinchem.2014.224907.

610 24. E. Picardi, G. Pesole, REDItools: High-throughput RNA editing detection made
611 easy. Bioinformatics (2013), doi:10.1093/bioinformatics/btt287.

612 25. J. Hadfield, C. Megill, S. M. Bell, J. Huddleston, B. Potter, C. Callender, P.
613 Sagulenko, T. Bedford, R. A. Neher, NextStrain: Real-time tracking of pathogen
614 evolution. Bioinformatics (2018), doi:10.1093/bioinformatics/bty407.

615 26. S. Song, L. Ma, D. Zou, D. Tian, C. Li, J. Zhu, M. Chen, A. Wang, Y. Ma, M. Li, X.
616 Teng, Y. Cui, G. Duan, M. Zhang, T. Jin, C. Shi, Z. Du, Y. Zhang, C. Liu, R. Li, J.
617 Zeng, L. Hao, S. Jiang, H. Chen, D. Han, J. Xiao, Z. Zhang, W. Zhao, Y. Xue, Y.
618 Bao, The global landscape of SARS-CoV-2 genomes, variants, and haplotypes in
619 2019nCoVR. bioRxiv (2020).

620 27. M. J. Abraham, T. Murtola, R. Schulz, S. Páll, J. C. Smith, B. Hess, E. Lindah,
621 Gromacs: High performance molecular simulations through multi-level parallelism
622 from laptops to supercomputers. SoftwareX (2015),
623 doi:10.1016/j.softx.2015.06.001.

624

Acknowledgement

The study was supported by the Department of Health and SEHA in Abu Dhabi, the United Arab Emirates and National Natural Science Foundation of China (31900487). We would like to acknowledge Xihui Chen and Fengliang Cui, Qinglong Wang, Shengchang Gu, Guoyang Xu from MGI for the fast installation of sequencing instruments, the G42 Huoyan laboratory members who contributed to the collection of samples, Dr. Joseph Mafofo and Inacio Pacheco for suggestions on the IRB application, professors Huachun Zou, Qianglin Fang and associated professors Huicui Feng, Jinqiu Yuan and Yawen Jiang from the school of public health (Shenzhen), Sun-Yat-Sen University, associated professor Jinqiu Yuan from the seventh affiliated hospital and Dr. Min Sum Park for helpful scientific discussion and suggestion in the study.

Author contributions

Conceptualization, S. Liu, W. Z; Methodology, J. L, S. Liu, R. Liu, P. W, K. L, P. L, L. L; Formal Analysis, R. Liu, P. W, D. L, W. H, S. Liu; Resources, S. M, T. M, Z. Y, X. M; Data Curation, R. Liu, N. K, M. F, H. K, J. Q, V. K; Writing - Original Fraft, S.Liu; Writing - Review & Editing, S.Liu, P. O, S. F, H. K, C.Y; Supervision, P. X, X. X, X. A, X. J, B. A, J. W, H. Y; Project Administration, T. M, F. C, N. Q, X. H and W. L; Funding Acquisition, A.K, W. L and S. Liu.

Funding

Department of Health of Abu Dhabi, UAE and National Natural Science Foundation of China (31900487).

Competing interests

The authors declare that they have no competing interests.

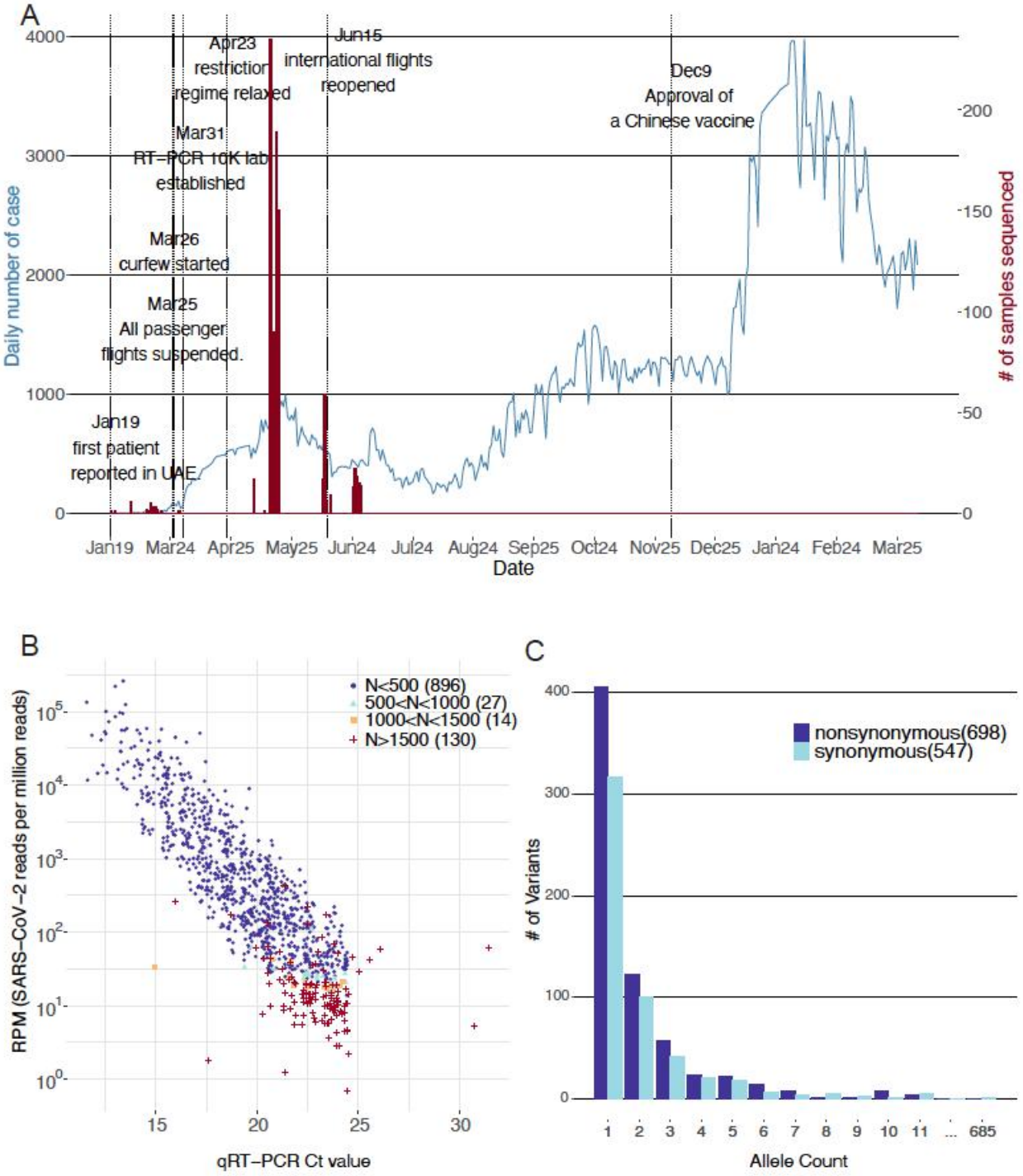

Figure 1. COVID-19 outbreak in the United Arab Emirates and the samples subjected for sequencing in this study. (A) Number of confirmed infected cases in the UAE (N=461,444) until Mar 31st 2021 was shown in the blue line and the number of subjects sequenced by meta-transcriptomic sequencing (N=1,067) was shown in the red

653 bars. Important dates reflecting governmental responses were marked in black text. (B)
654 Assembly quality of the 1,067 viral genomes as a function of the RT-PCR Ct value and
655 SARS-CoV-2 reads per million sequencing reads. Color represents assembly quality
656 stratified by the number of gaps. (C) Allele frequency spectrum of the 1,245 genetic
657 variants identified from the 896 assemblies with less than 2% gaps.

658

659

660

661

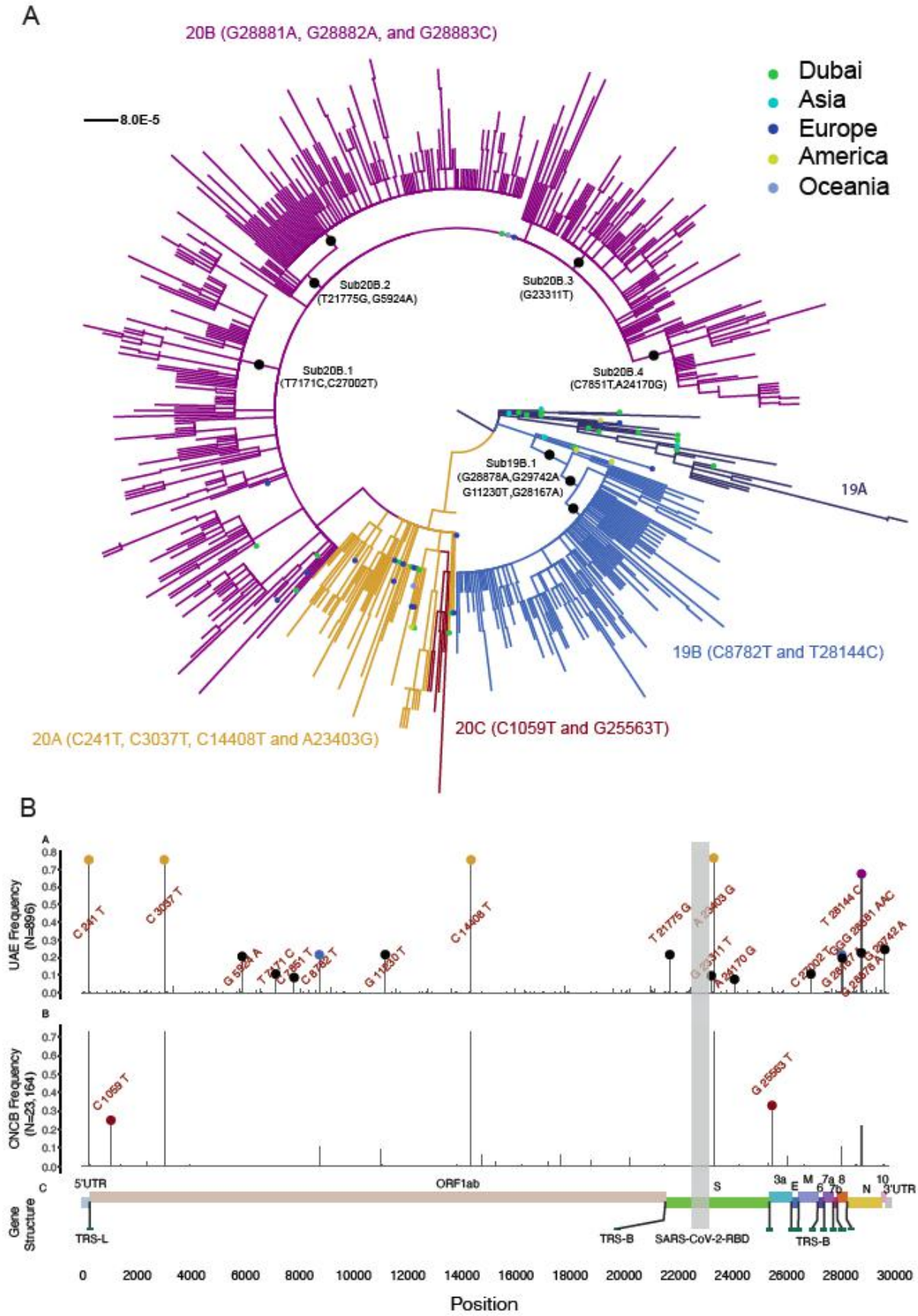
A
20B (G28881A, G28882A, and G28883C)
8.0E-5
Dubai
Asia
Europe
America
Oceania
Sub20B.2
(T21775G,G5924A)
Sub20B.3
(G23311T)
Sub20B.1
(T7171C,C27002T)
Sub20B.4
(C7851T,A24170G)
Sub19B.1
(G28878A,G29742A
G11230T,G28167A)
19A
19B (C8782T and T28144C)
20A (C241T, C3037T, C14408T and A23403G)
20C (C1059T and G25563T)
B
UAE Frequency
(N=896)
C 241 T
C 3037 T
C 14408 T
T 21775 G
A 23403 G
G 23311 T
A 24170 G
T 28144 C
C 1059 T
G 25563 T
GNCB Frequency
(N=23,164)
Gene
Structure
5'UTR
ORF1ab
S
3a
E
M
6
7a
7b
8
N
10
3'UTR
TRS-L
TRS-B
SARS-CoV-2-RBD
TRS-B
0
2000
4000
6000
8000
10000
12000
14000
16000
18000
20000
22000
24000
26000
28000
30000
Position

662

663 **Figure 2. Phylogenetic analysis of the sequenced UAE viral population during May**
664 **and June.** (A). Maximum likelihood tree of the 637 unique viral genomes with less than
665 2% gaps and 52 closest relatives from GISAID. Each line indicates a sample colored by
666 the five dominant viral clades worldwide, annotated with the clade definitive genetic
667 variation. The subclade-definitive genetic variations were also marked in black. The
668 closest relatives from GISAID were marked by a dot colored by geographical district
669 reported for the viral sample. (B). Comparison of the alternative allele frequency of the
670 1,245 viral genetic variants between the 896 high quality UAE viral genomes and the
671 23,164 viral genomes from the globe downloaded from the China National Center for
672 Bioinformation. Nomenclature of the clades was detailed in Supplementary Notes.

673

674

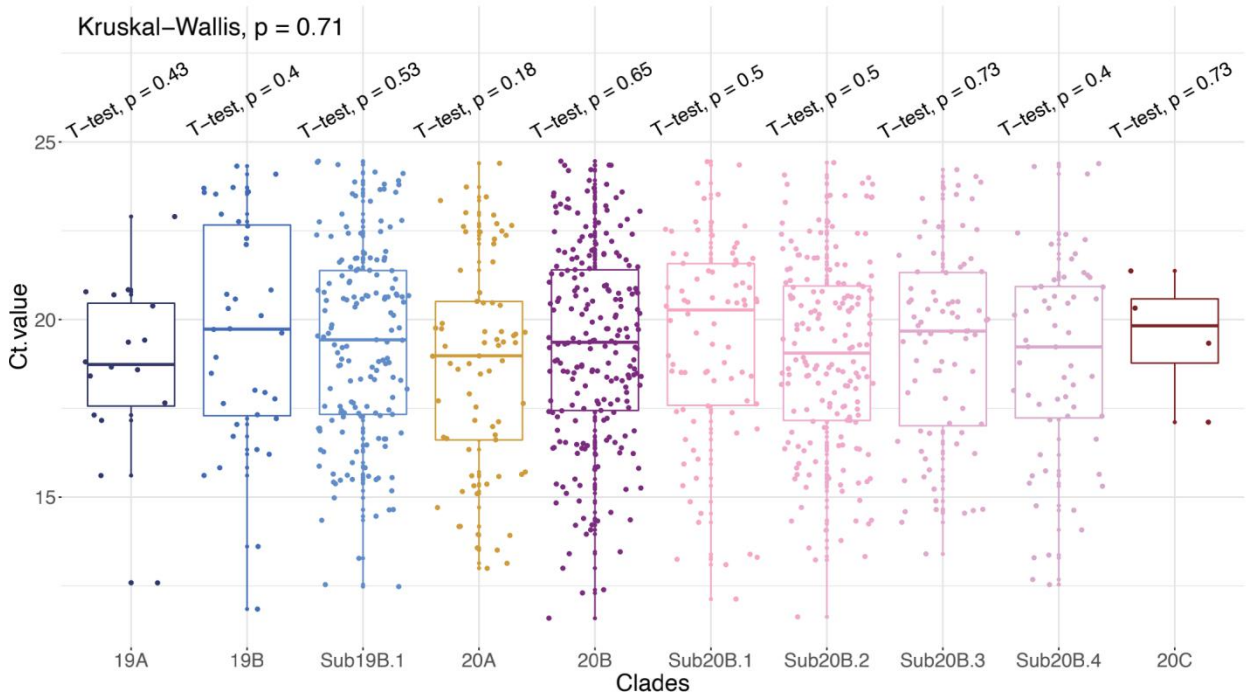

675

676 **Figure 3. Functional analysis of the unique variants and subclade in the UAE**
677 **samples.** RT-qPCR Ct value distribution for samples in each of the five dominant clades
678 and five subclades. Shown is the p-value using Kruskai-Wallis test and p-value by
679 performing T-test comparing the Ct value for patients carrying certain clade or subclade
680 virus strains with the rest of the patients who didn't carry the virus belong to a specific
681 clade or subclade.

682

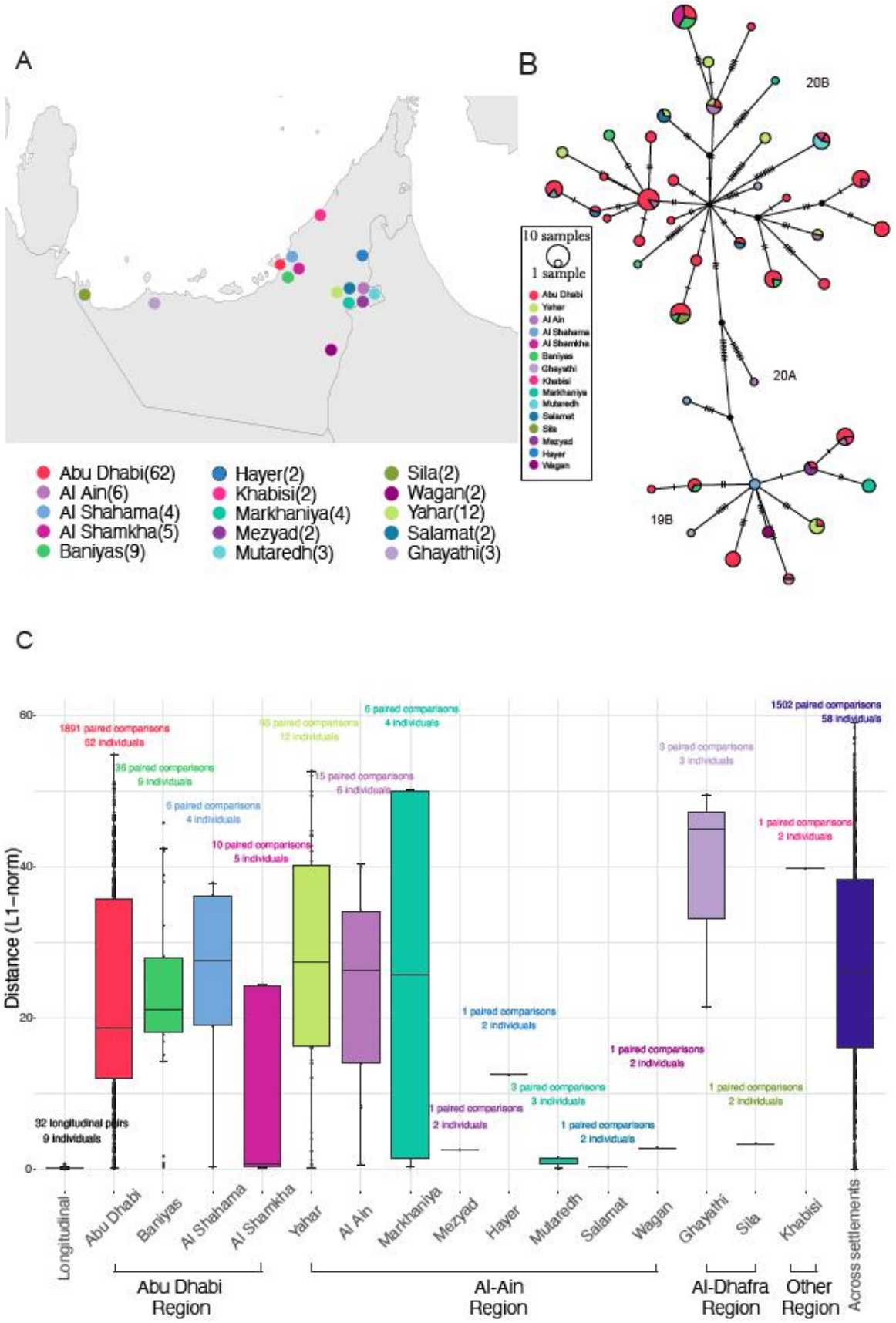
A
Abu Dhabi(62)
Al Ain(6)
Al Shahama(4)
Al Shamkha(5)
Baniyas(9)
Hayer(2)
Khabisi(2)
Markhaniya(4)
Mezyad(2)
Mutaredh(3)
Sila(2)
Wagan(2)
Yahar(12)
Salamat(2)
Ghayathi(3)
B
20B
20A
19B
10 samples
1 sample
Abu Dhabi
Yahar
Al Ain
Al Shahama
Al Shamkha
Baniyas
Ghayathi
Khabisi
Markhaniya
Mutaredh
Salamat
Sila
Mezyad
Hayer
Wagan
C
Distance (L1−norm)
0
20
40
60
1891 paired comparisons
62 individuals
36 paired comparisons
9 individuals
6 paired comparisons
4 individuals
10 paired comparisons
5 individuals
66 paired comparisons
12 individuals
15 paired comparisons
6 individuals
6 paired comparisons
4 individuals
1 paired comparisons
2 individuals
3 paired comparisons
3 individuals
1 paired comparisons
2 individuals
1 paired comparisons
2 individuals
3 paired comparisons
3 individuals
1 paired comparisons
2 individuals
1 paired comparisons
2 individuals
1502 paired comparisons
58 individuals
32 longitudinal pairs
9 individuals
Longitudinal
Abu Dhabi
Baniyas
Al Shahama
Al Shamkha
Yahar
Al Ain
Markhaniya
Mezyad
Hayer
Mutaredh
Salamat
Wagan
Ghayathi
Sila
Khabisi
Across settlements
Abu Dhabi Region
Al-Ain Region
Al-Dhafra Region
Other Region

683

Figure 4. Human-to-human transmission across settlements. (A). Geographical distribution of 120 viral samples with settlement level information in the Abu Dhabi city. (B). Transmission network of the 120 samples colored by settlements. (C). L1-norm genetic distance for longitudinal samples, samples from the same settlements, and samples from different settlements. Among the 130 samples that report settlement level geographical location in Table S5, 10 samples were not displayed because only one sample were collected from that settlement.

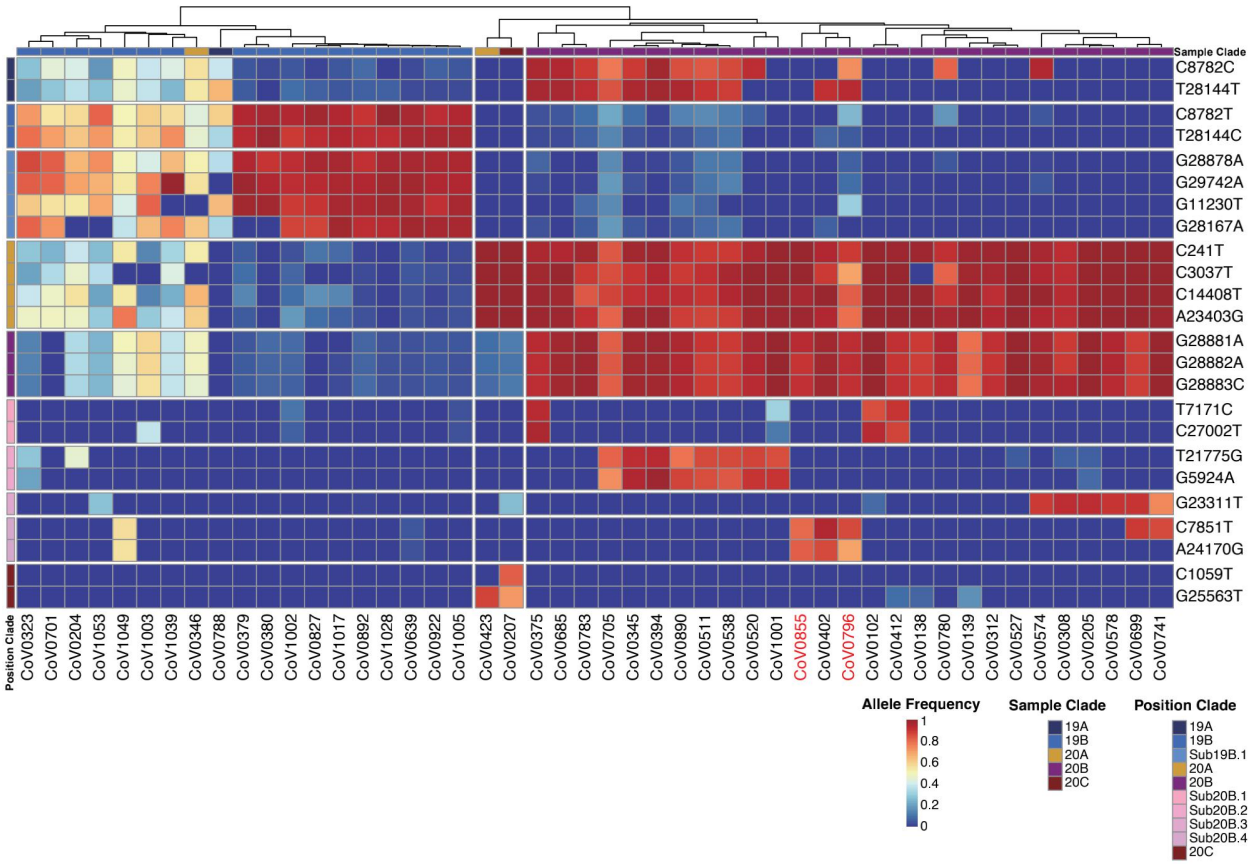

Figure 5. Co-infection with multiple SARS-CoV-2 variants. Evidence for human-to-human transmission of multiple SARS-CoV-2 variants were established using the clade and sub-clade definitive viral genetic variants. Columns display the de-identified sample ID that carried more than one SARS-CoV-2 viral variants in the nasopharyngeal swab sampling (N=48). Color bar shows the viral clade assigned to the individual, according to the consensus viral sequence, reflecting the dominant clade in one sample. Rows indicate the eleven clade- definitive and eleven sub-clade definitive variants. Heatmap color, ranging from red to blue, suggests the allelic proportion of the derived allele of the iSNV. The ID of two longitudinal samples were marked in red.

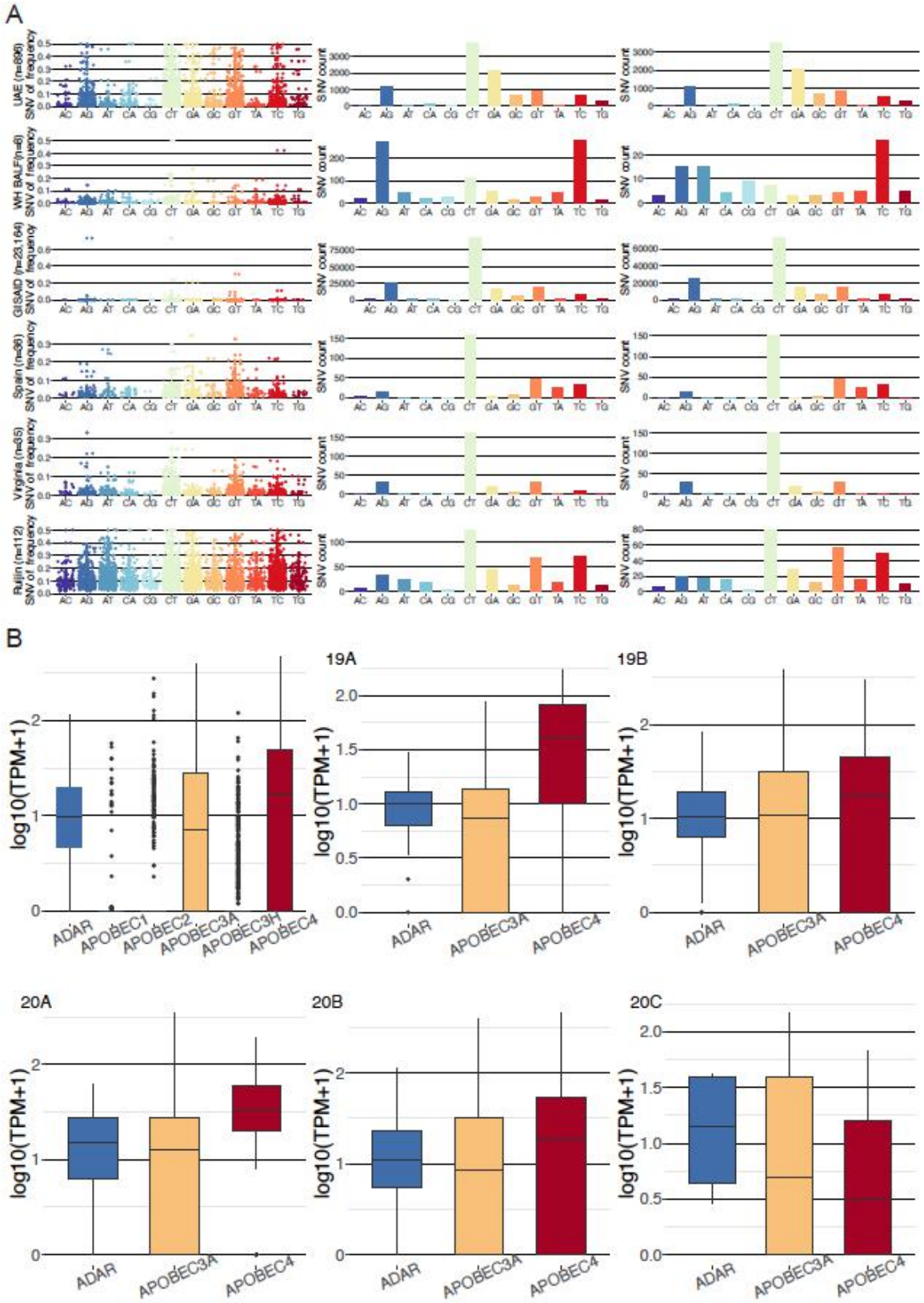
A
UAE (n=896)
WH BALF(n=6)
GISAID (n=23,164)
Spain (n=36)
Virginia (n=35)
Rujin (n=112)
SNV of frequency
SNV count
AC AG AT CA CG CT GA GC GT TA TC TG
B
log10(TPM+1)
ADAR
APOBEC1
APOBEC2
APOBEC3A
APOBEC3H
APOBEC4
19A
19B
20A
20B
20C

704 **Figure 6. Human innate immune response to SARS-CoV-2 mediated by the ADAR**
705 **and APOBEC gene families.** (A). Allelic faction (Column 1), the number of mutations
706 (Column 2) and the number of recurrent mutations (Column 3) for ten mutation types for
707 six studies arranged by row. UAE: 896 nasal swab samples collected in our study;
708 GISAID: 23,164 viral sequences collected; Spain: 36 nasal swab samples collected in
709 Spain; Virginia: 35 nasal swab samples collected in Virginia and 112 nasal swab
710 samples collected in Ruijin hospital in Shanghai city, China. (B). Host *ADAR* and
711 *APOBEC* gene expression (logarithm of transcript per million) in the nasal swab samples
712 for all and for each of the five clades.

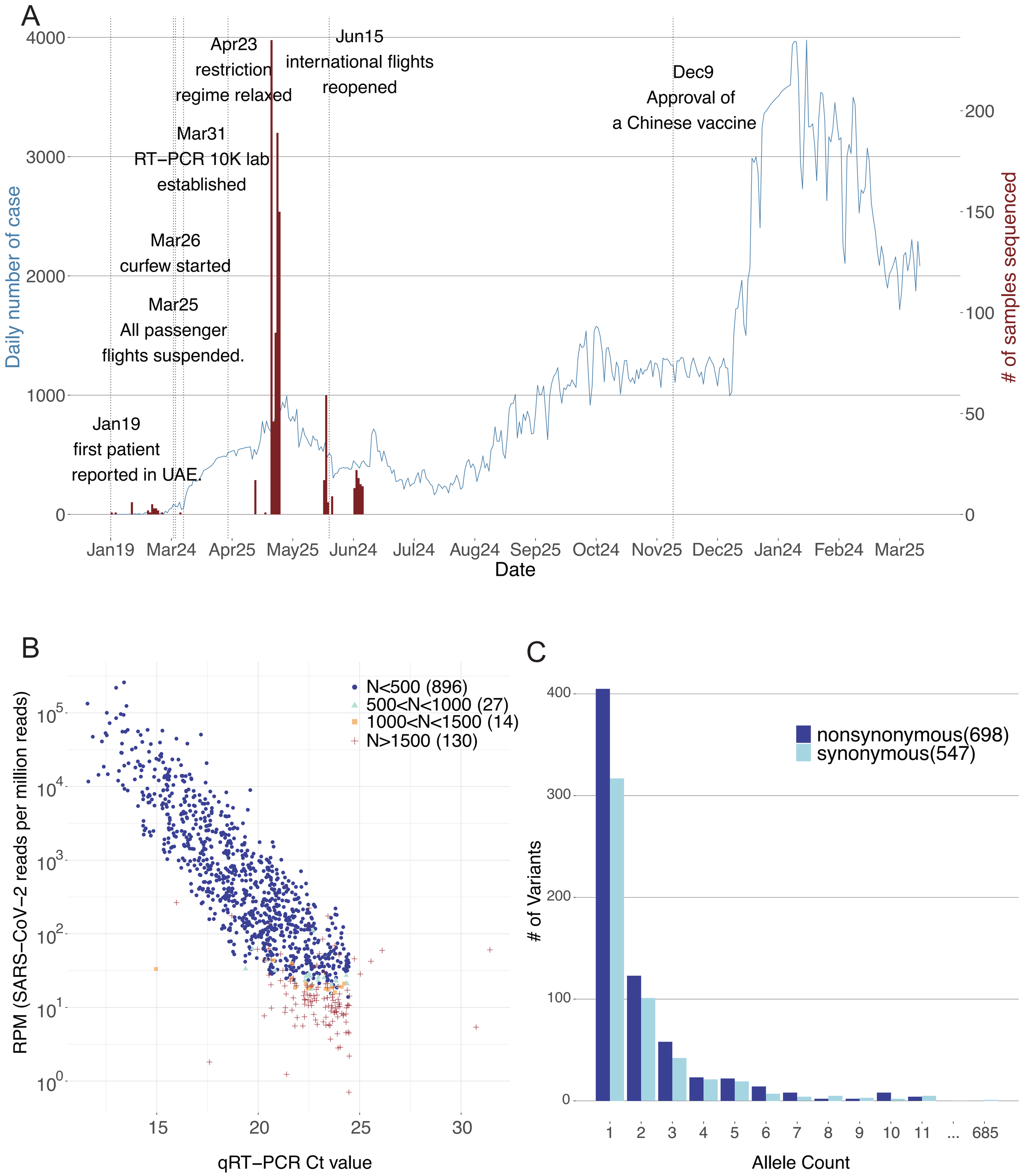
A
Daily number of case
# of samples sequenced
Jan19
first patient
reported in UAE.
Mar25
All passenger
flights suspended.
Mar26
curfew started
Mar31
RT−PCR 10K lab
established
Apr23
restriction
regime relaxed
Jun15
international flights
reopened
Dec9
Approval of
a Chinese vaccine
Date
B
N<500 (896)
500<N<1000 (27)
1000<N<1500 (14)
N>1500 (130)
RPM (SARS−CoV−2 reads per million reads)
qRT−PCR Ct value
C
nonsynonymous(698)
synonymous(547)
# of Variants
Allele Count

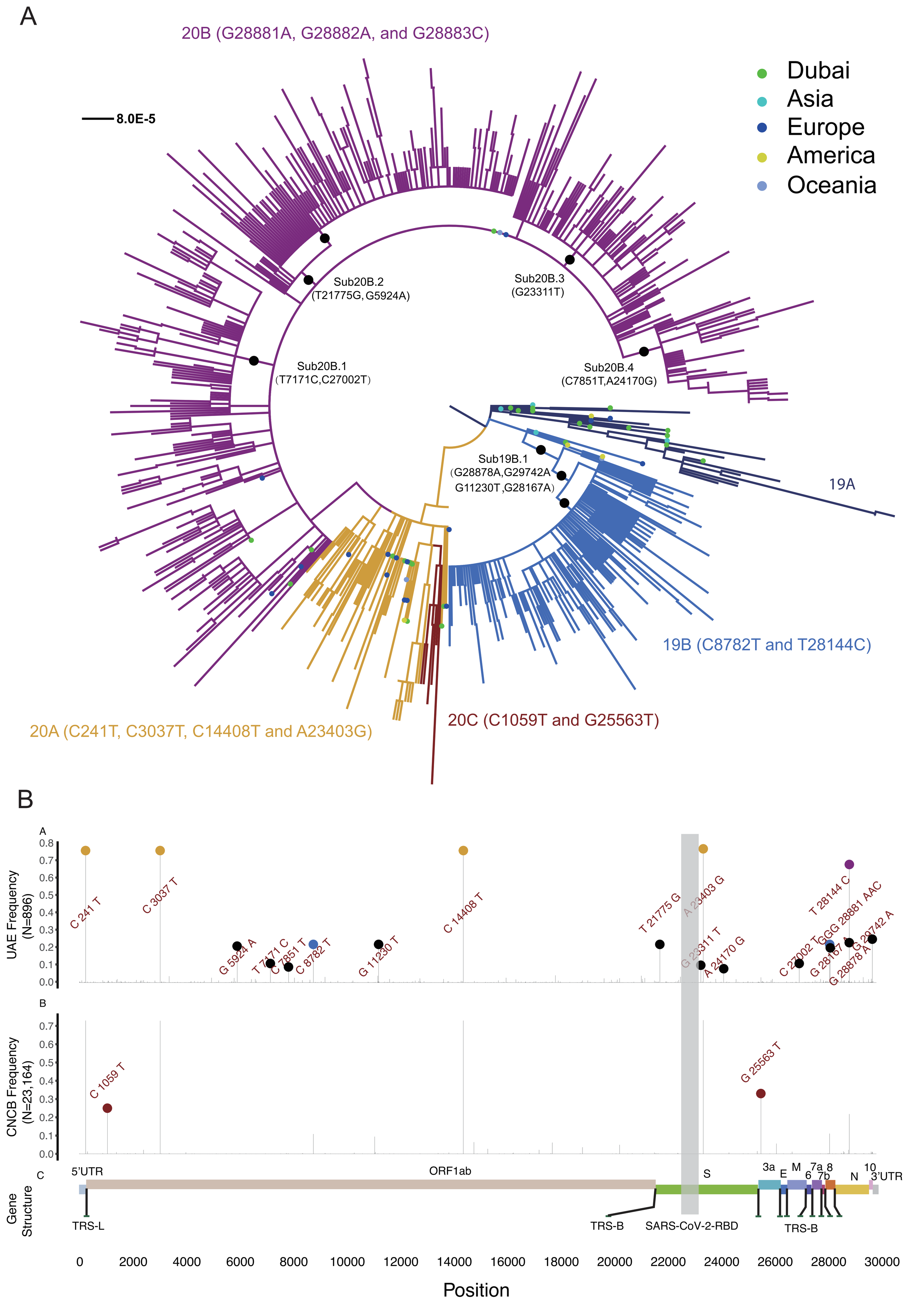
A
20B (G28881A, G28882A, and G28883C)
8.0E-5
Dubai
Asia
Europe
America
Oceania
Sub20B.2
(T21775G, G5924A)
Sub20B.3
(G23311T)
Sub20B.1
(T7171C,C27002T)
Sub20B.4
(C7851T,A24170G)
Sub19B.1
(G28878A,G29742A
G11230T,G28167A)
19A
19B (C8782T and T28144C)
20C (C1059T and G25563T)
20A (C241T, C3037T, C14408T and A23403G)
B
A
UAE Frequency
(N=896)
C 241 T
C 3037 T
G 5924 A
T 7171 C
C 7851 T
C 8782 T
G 11230 T
C 14408 T
T 21775 G
A 23403 G
G 23311 T
A 24170 G
C 27002 T
G 28167 A
G 28878 A
G 29742 A
T 28144 C
GGG 28881 AAC
B
CNCB Frequency
(N=23,164)
C 1059 T
G 25563 T
C
Gene
Structure
5'UTR
ORF1ab
S
3a
E
M
6
7a
7b
8
N
10
3'UTR
TRS-L
TRS-B
SARS-CoV-2-RBD
TRS-B
0
2000
4000
6000
8000
10000
12000
14000
16000
18000
20000
22000
24000
26000
28000
30000
Position

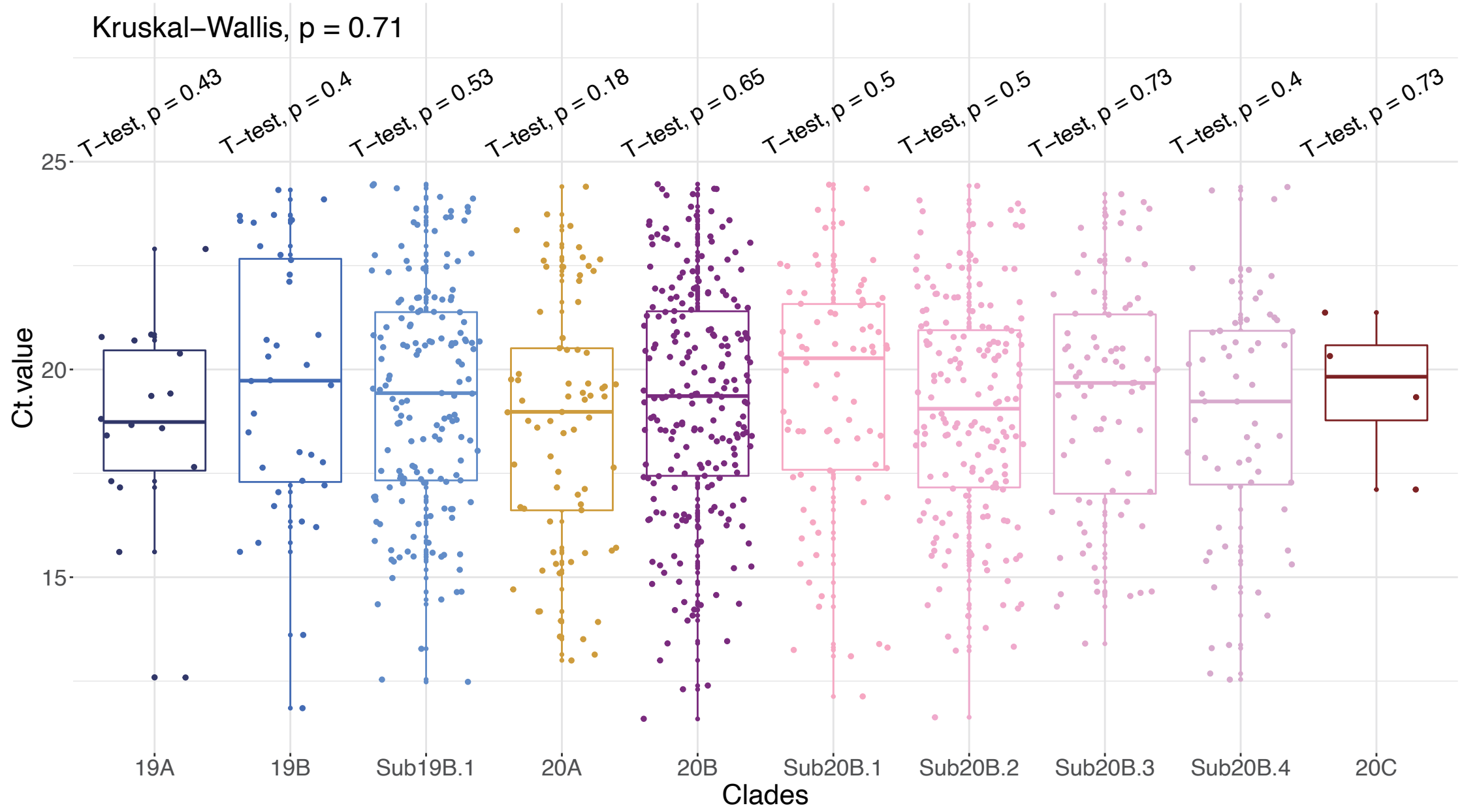
Kruskal–Wallis, p = 0.71
T–test, p = 0.43
T–test, p = 0.4
T–test, p = 0.53
T–test, p = 0.18
T–test, p = 0.65
T–test, p = 0.5
T–test, p = 0.5
T–test, p = 0.73
T–test, p = 0.4
T–test, p = 0.73
25
20
15
Ct.value
19A
19B
Sub19B.1
20A
20B
Sub20B.1
Sub20B.2
Sub20B.3
Sub20B.4
20C
Clades

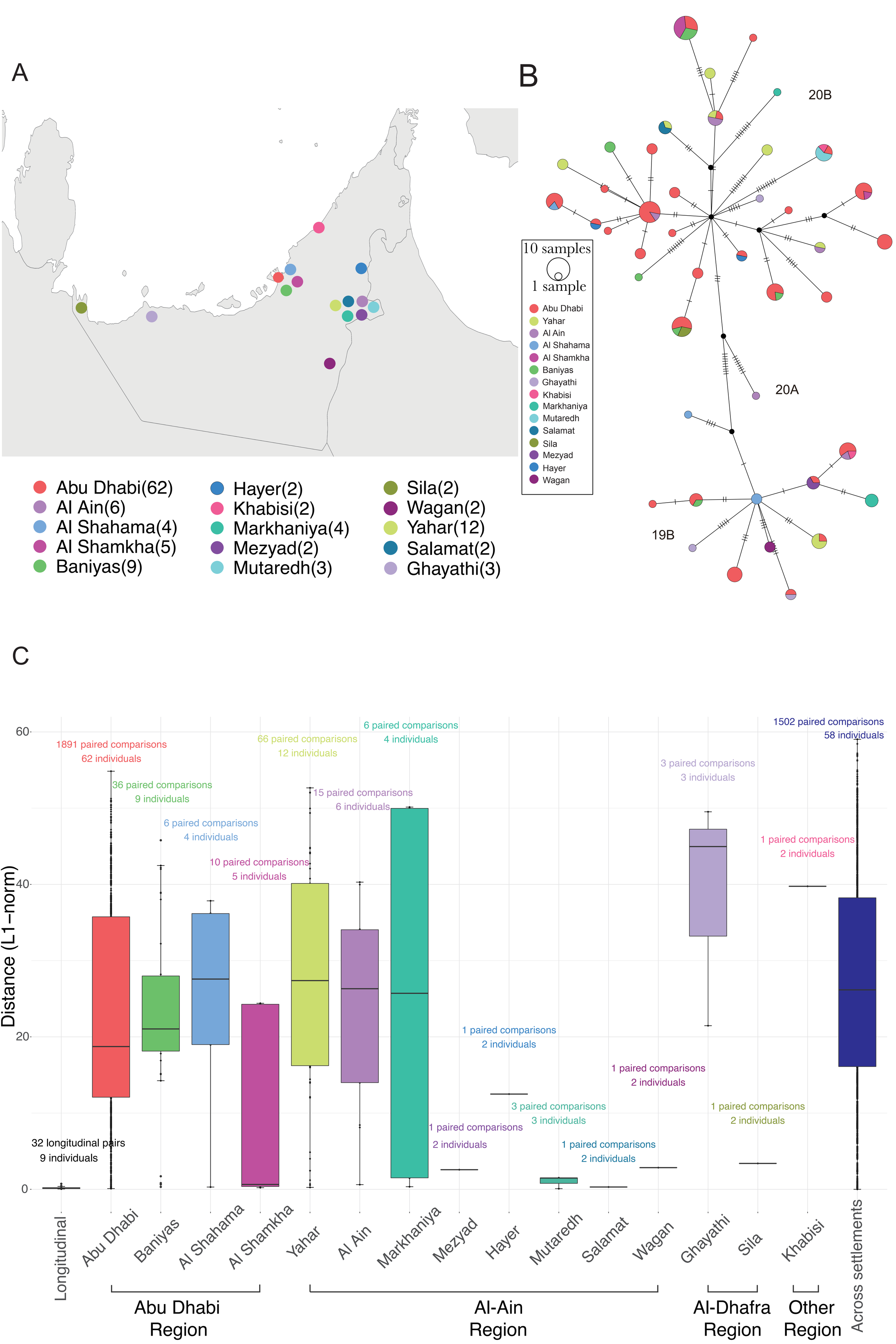
A
B
C
10 samples
1 sample
Abu Dhabi
Yahar
Al Ain
Al Shahama
Al Shamkha
Baniyas
Ghayathi
Khabisi
Markhaniya
Mutaredh
Salamat
Sila
Mezyad
Hayer
Wagan
20B
20A
19B
Abu Dhabi(62)
Al Ain(6)
Al Shahama(4)
Al Shamkha(5)
Baniyas(9)
Hayer(2)
Khabisi(2)
Markhaniya(4)
Mezyad(2)
Mutaredh(3)
Sila(2)
Wagan(2)
Yahar(12)
Salamat(2)
Ghayathi(3)
Distance (L1−norm)
60
40
20
0
1891 paired comparisons
62 individuals
36 paired comparisons
9 individuals
6 paired comparisons
4 individuals
10 paired comparisons
5 individuals
66 paired comparisons
12 individuals
15 paired comparisons
6 individuals
6 paired comparisons
4 individuals
1 paired comparisons
2 individuals
3 paired comparisons
3 individuals
1 paired comparisons
2 individuals
1 paired comparisons
2 individuals
1 paired comparisons
2 individuals
3 paired comparisons
3 individuals
1 paired comparisons
2 individuals
1502 paired comparisons
58 individuals
32 longitudinal pairs
9 individuals
Longitudinal
Abu Dhabi
Baniyas
Al Shahama
Al Shamkha
Yahar
Al Ain
Markhaniya
Mezyad
Hayer
Mutaredh
Salamat
Wagan
Ghayathi
Sila
Khabisi
Across settlements
Abu Dhabi Region
Al-Ain Region
Al-Dhafra Region
Other Region

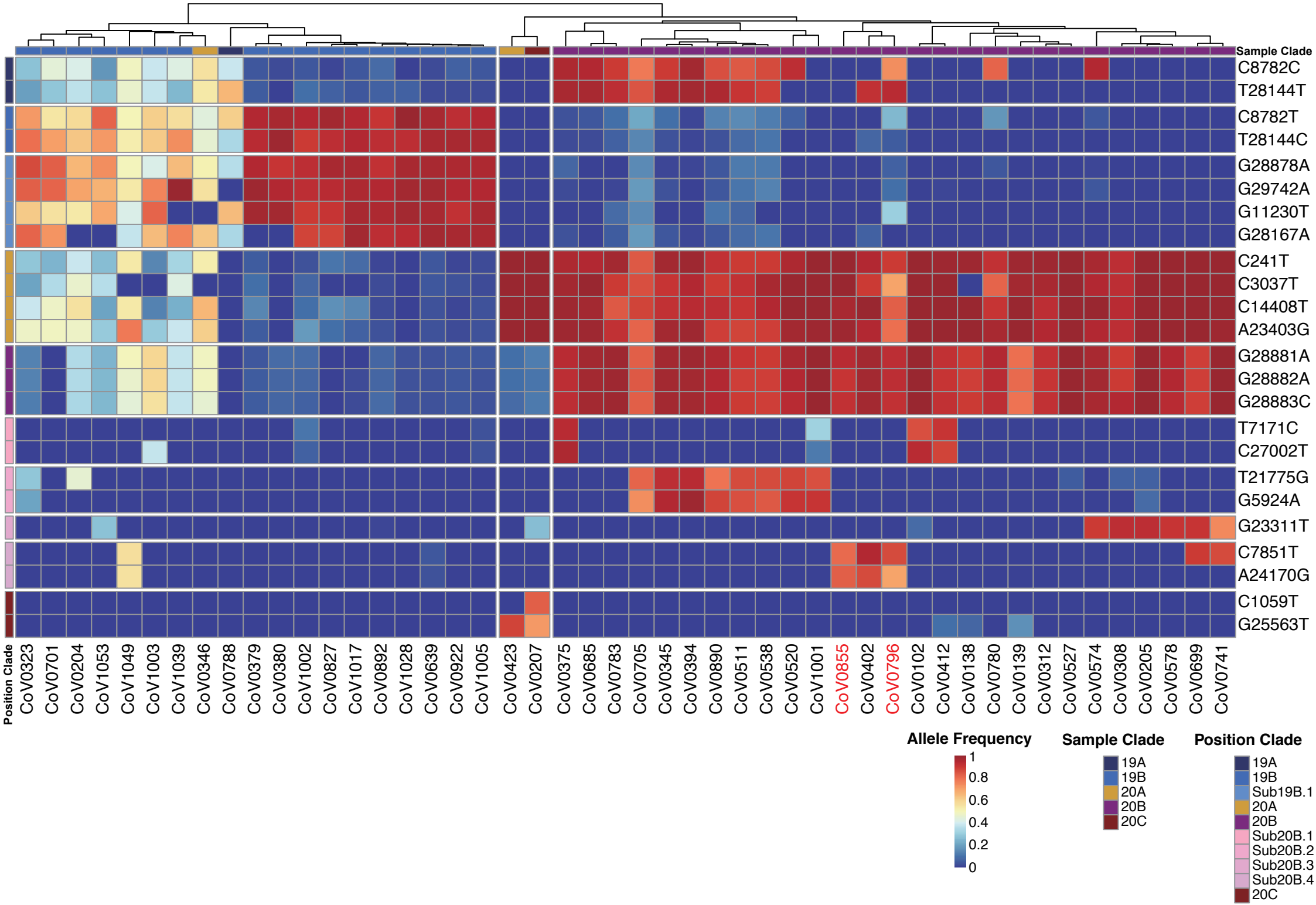
Sample Clade
C8782C
T28144T
C8782T
T28144C
G28878A
G29742A
G11230T
G28167A
C241T
C3037T
C14408T
A23403G
G28881A
G28882A
G28883C
T7171C
C27002T
T21775G
G5924A
G23311T
C7851T
A24170G
C1059T
G25563T
Position Clade
CoV0323
CoV0701
CoV0204
CoV1053
CoV1049
CoV1003
CoV1039
CoV0346
CoV0788
CoV0379
CoV0380
CoV1002
CoV0827
CoV1017
CoV0892
CoV1028
CoV0639
CoV0922
CoV1005
CoV0423
CoV0207
CoV0375
CoV0685
CoV0783
CoV0705
CoV0345
CoV0394
CoV0890
CoV0511
CoV0538
CoV0520
CoV1001
CoV0855
CoV0402
CoV0796
CoV0102
CoV0412
CoV0138
CoV0780
CoV0139
CoV0312
CoV0527
CoV0574
CoV0308
CoV0205
CoV0578
CoV0699
CoV0741
Allele Frequency
1
0.8
0.6
0.4
0.2
0
Sample Clade
19A
19B
20A
20B
20C
Position Clade
19A
19B
Sub19B.1
20A
20B
Sub20B.1
Sub20B.2
Sub20B.3
Sub20B.4
20C

A

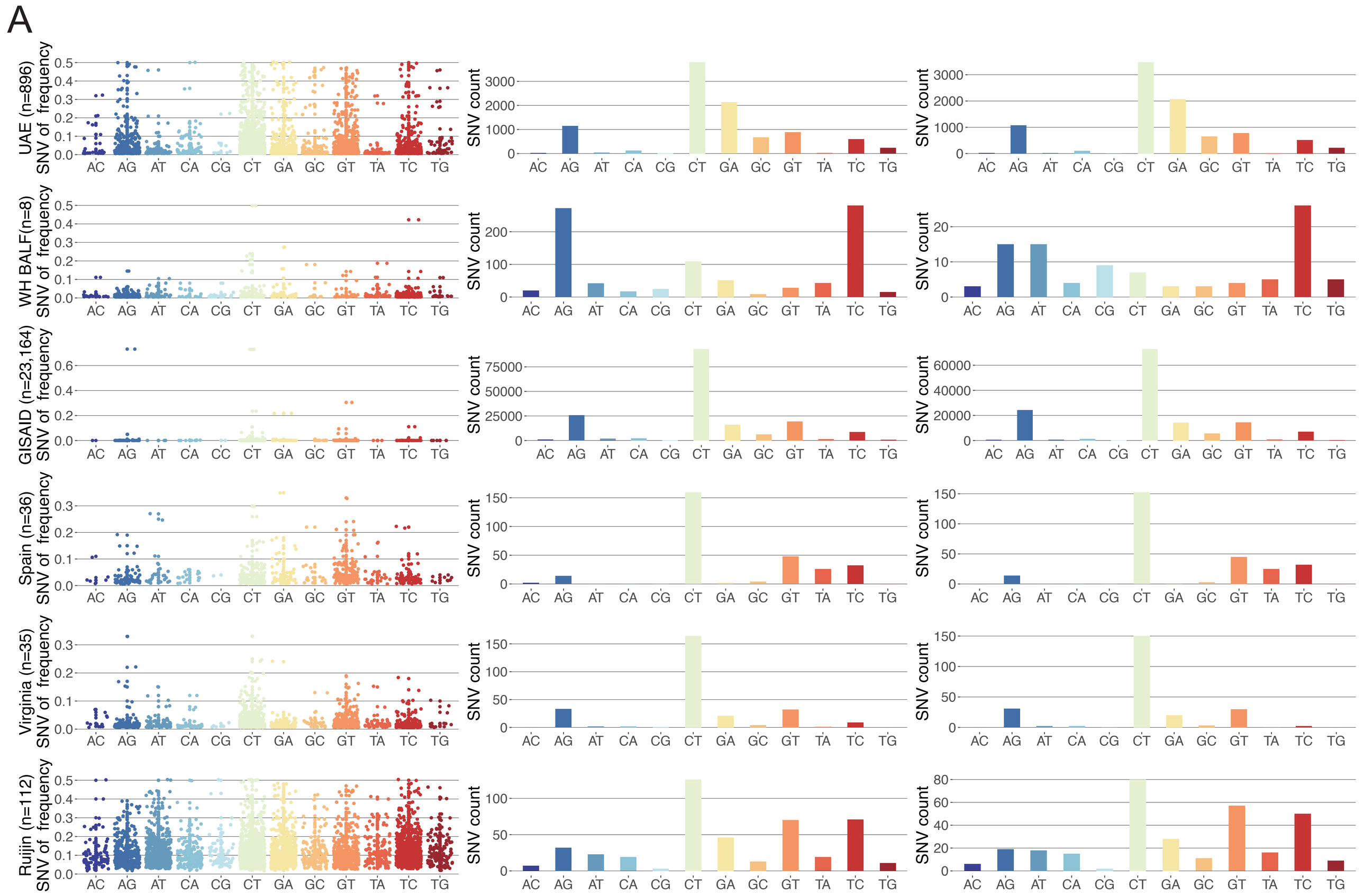
UAE (n=896)
WH BALF(n=8)
GISAID (n=23,164)
Spain (n=36)
Virginia (n=35)
Ruijin (n=112)
SNV of frequency
SNV count
AC AG AT CA CG CT GA GC GT TA TC TG

B

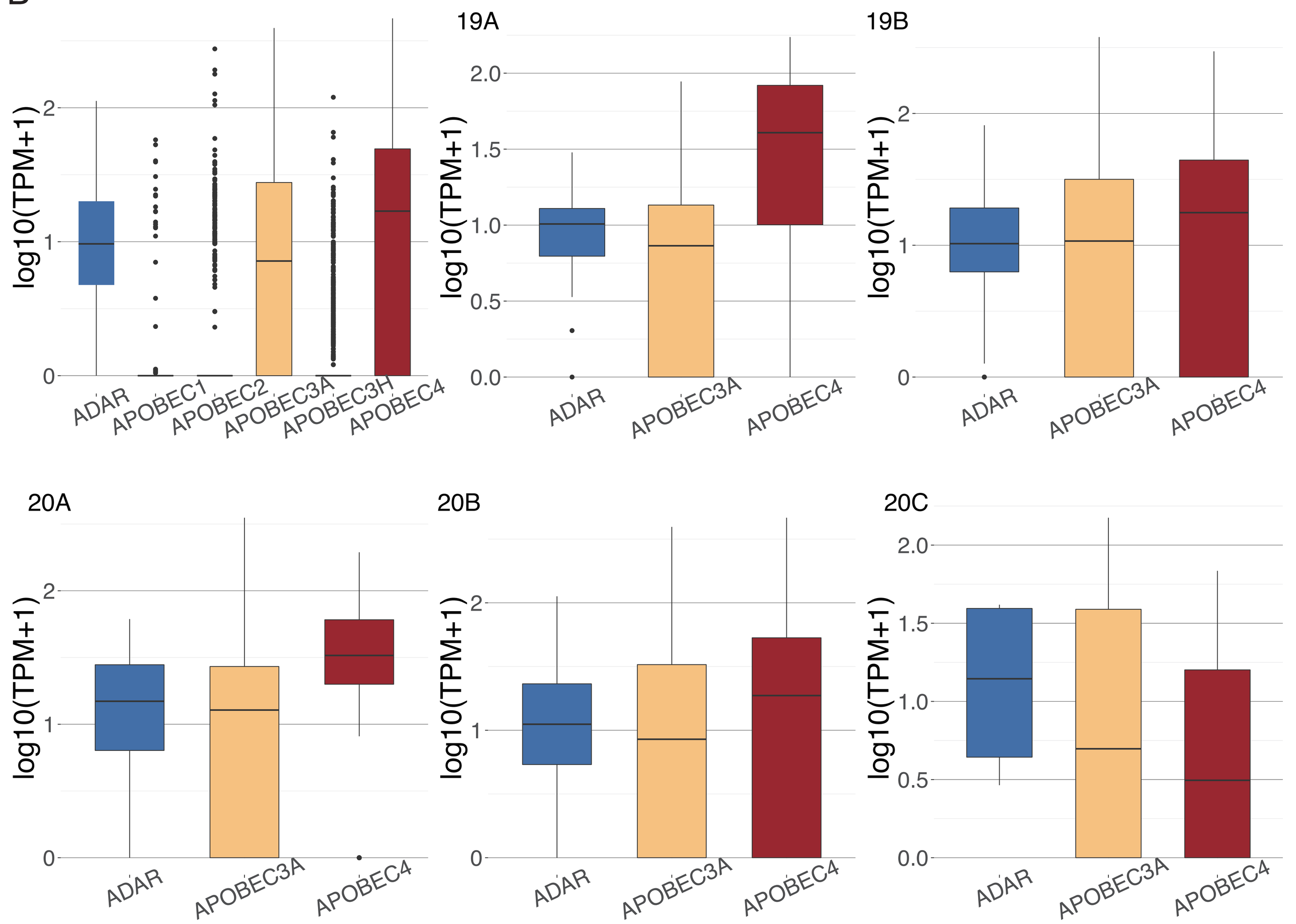
19A
19B
20A
20B
20C
log10(TPM+1)
ADAR
APOBEC1
APOBEC2
APOBEC3A
APOBEC3H
APOBEC4